MHD AIR HEATER DEVELOPMENT TECHNOLOGY

Technical Progress Report
For the Period
July 1, 1980 - September 30, 1980

Prepared for

United States Department of Energy
Division of Magnetohydrodynamics
Under Contract # DE-AC01-80ET15602

Prepared by

FluiDyne Engineering Corporation
5900 Olson Memorial Highway
Minneapolis, Minnesota 55422

FluiDyne Job 1228
November, 1980

DISCLAIMER

NOTICE

This report was prepared to document work sponsored by the United States Government. Neither the United States nor its agent, the United States Department of Energy, nor any Federal employees, nor any of their contractors, subcontractors or their employees, makes any warranty, express or implied, or assumes any legal liability or responsibility for the accuracy, completeness, or usefulness of any information, apparatus, product or process disclosed, or represents that its use would not infringe privately owned rights.

TABLE OF CONTENTS

1.0 OBJECTIVE AND SCOPE OF WORK

Work to be done under this Contract will continue the technology development of the directly-fired high temperature air heater (HTAH) for MHD power plants. The work will extend the efforts begun under previous ERDA/DOE contracts, the most recent being Contract DEAC01-78ET10814. The Statement of Work specifies work to be done under three tasks as described in the following.

Task 1 - Materials Selection, Evaluation, and Development

The objective of this task is to continue development of ceramic materials technology for the directly-fired HTAH. The scope of the work under Task 1 will include compilation of materials data, materials selection for testing and design studies, materials property determination, liaison with refractory manufacturers and other organizations to encourage development of materials and fabrication technology, establishment of preliminary HTAH material specifications, analyses of test materials, and development of criteria for thermal stress limits for crack-tolerant refractory materials.

Task 2 - Operability, Performance, and Materials Testing

The objectives of this task are to demonstrate the technical feasibility of operating a directly-fired HTAH (including both the heater matrix and valves), to continue obtaining information on life and corrosion resistance of HTAH materials, and to obtain design information for full-scale studies and future design work. The scope of the work will include tests in the Matrix Test Facility (MTF) and Valve Test Facility (VTF) built and operated under contracts EX-76-C-01-2254 and DE-AC01-78ET10814, emissions measurements in the MTF and VTF, design of a dilatometer for performing creep measurements in the directly-fired HTAH environment, and characterization of the effluent air stream from the MTF.

Task 3 - Full-Scale Design Concepts

The objectives of this task are to begin the identification of HTAH control requirements and control system needs, and to continue full-scale study efforts incorporating updated materials and design information in order to identify development needs for the HTAH development program. The scope of the work will include size/cost analyses and parametric studies of design options using a size/cost code and other computer codes developed and refined under Contracts EX-76-C-01-2254 and DE-AC01-78ET10814, dynamic HTAH system performance calculations using the SCAMP (System Cyclic Analysis of Multiple Preheaters) computer code developed under Contract DE-AC01-78ET10814, preparation of system layouts and cost estimates, screening and definition of control systems and determination of operating methods, definition of requirements for a future test facility to test matrix support concepts at nearly full-scale, and development of design concepts for alternative heater systems and electrical isolation of the air duct from the MHD combustor.

U.S. DEPARTMENT OF ENERGY

FORM DOE 535
(1/78)

MILESTONE SCHEDULE AND STATUS REPORT

FORM APPROVED
OMB NO. 85-R-0148

1. Contract Identification	2. Reporting Period	3. Contract Number
MHD AIR HEATER TECHNOLOGY	1 July 1980 through 30 Sept. 1980	DE-AC01-80ET15602

4. Contractor (name, address)	5. Contract Start Date	6. Contract Completion Date
FluiDyne Engineering Corporation 5900 Olson Memorial Highway Minneapolis, MN 55422	November 26,1979	November 25, 1980

7. Identification Number	8. Reporting Category (e.g., contract line item or work breakdown structure element)	9. Fiscal Years and Months	10. Percent Complete	
			a) Planned	b) Actual
1.1.1	Material Selection			100
1.1.2	Property Determination			90
1.1.3	Liaison			90
1.1.4	Specifications			40
1.1.5	Materials Analyses			40
1.1.6	Thermal Stress Criteria			75
1.2.1.1	MTF Inst./Data Acq.			100
1.2.1.2	MTF Modifications			100
1.2.1.3	MTF Testing			10
1.2.1.4	MTF Analysis/Reporting			0
1.2.2.1	VTF Inst./Data Acq.			100
1.2.2.2	VTF Modifications			100
1.2.2.3	VTF Testing			100
1.2.2.4	VTF Analysis/Reporting			80

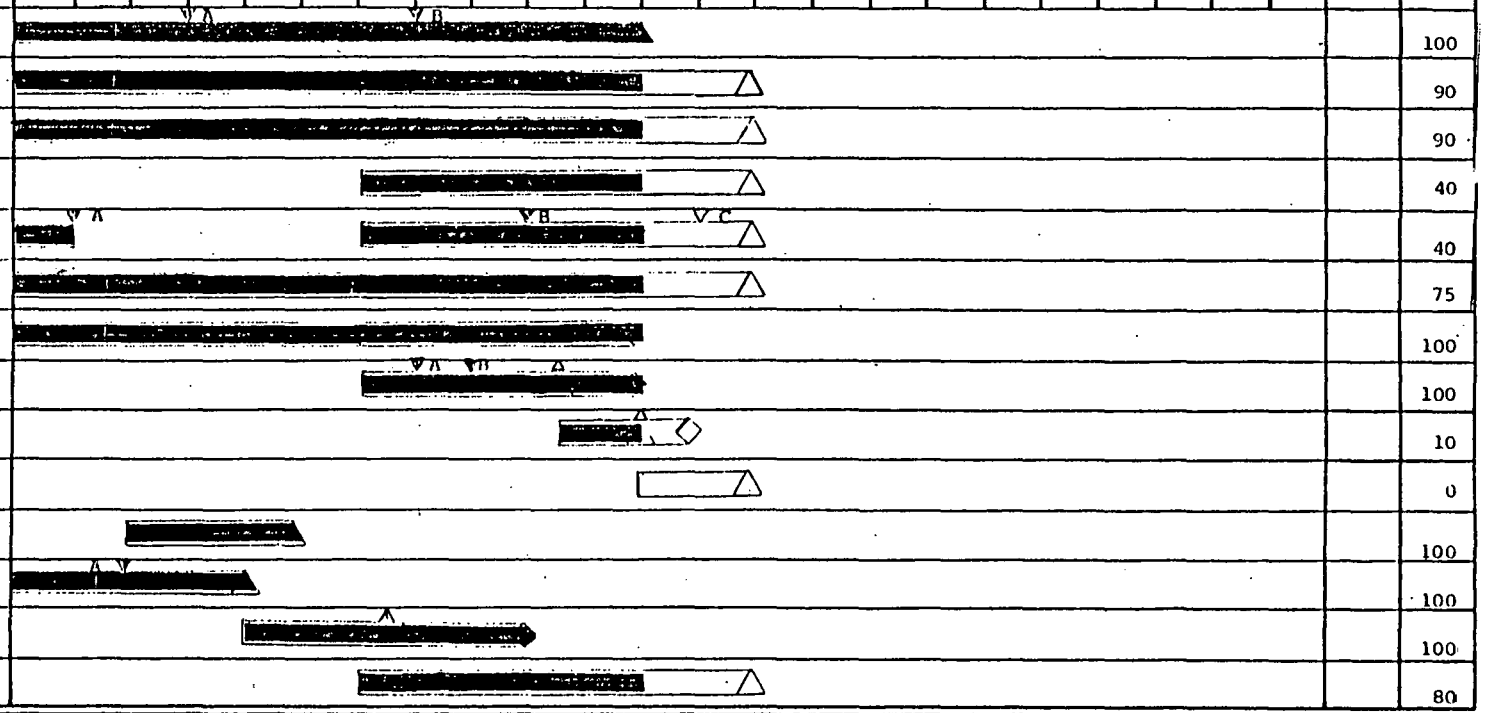

11. Remarks

Detail by WBS

12. Signature of Contractor's Project Manager and Date

M. J. McLaughlin 11-5-80

13. Signature of Government Technical Representative and Date

FORM DOE 536
(1/78)

U.S. DEPARTMENT OF ENERGY

MIL ...TONE SCHEDULE AND STATUS REPORT

FORM APPROVED OMB NO. 38-R-0188

1. Contract Identification	2. Reporting Period	3. Contract Number
MHD AIR HEATER TECHNOLOGY	1 July 1980 through 30 Sept. 1980	DE-AC01-80ET15602

4. Contractor (name, address)	5. Contract Start Date	6. Contract Completion Date
FluiDyne Engineering Corporation 5900 Olson Memorial Highway Minneapolis, MN 55422	November 26,1979	November 25, 1980

7. Identification Number	8. Reporting Category (e.g., contract line item or work breakdown structure element)	9. Fiscal Years and Months	10. Percent Complete a) Planned	10. Percent Complete b) Actual
1.2.3	Emissions Measurements			30
1.2.4	Creep Testing Apparatus			100
1.2.5	Effluent Air Stroam			30
1.3.1	Size/Cost			100
1.3.2	SCAMP			100
1.3.3	Layout Drawings			80
1.3.4	Cost Estimates			30
1.3.5	Control Systems			100
1.3.6	Matrix Support Test Facility			40
1.3.7	Alternative Heater Systems			40
1.3.8	Electrical Isolation			100

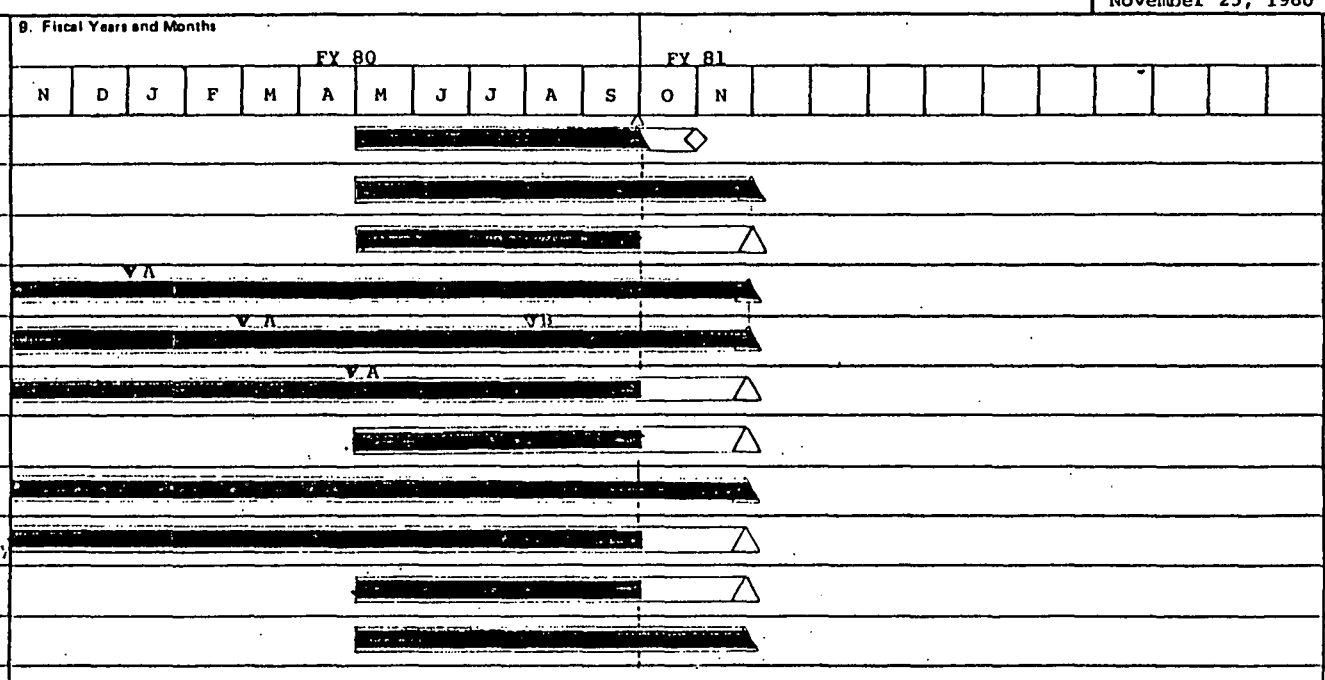

11. Remarks
Detail by WBS

12. Signature of Contractor's Project Manager and Date	13. Signature of Government Technical Representative and Date
S. McGowan 11-5-80	

MILESTONE LOG

Identification Number	Description	Completion Date Planned	Completion Date Actual	Comments
1.1.1A	Select. Matls for Full-Scale	Jan 80	Jan 80	
1.1.1B	Select. Matls. for Matrix Test	May 80	Jun 80	Addt'l matl's selected
1.1.1	Materials Selection	Sep 80	Sep 80	
1.1.2	Property Determinations	Nov 80		
1.1.3	Liaison	Nov 80		
1.1.4	Specifications	Nov 80		
1.1.5A	Analysis of Matrix and Valve Test Samples. Heat 202, VTF 1&2	Dec 79	Dec 79	
1.1.5B	Analysis of Valve Test Samples	July 80		
1.1.5C	Analysis of Matrix Test Samples	Oct 80		
1.1.5	Materials Samples Analyses	Nov 80		
1.1.6	Thermal Stress Criteria	Nov 80		
1.2.1.1	Instrumentation/Data Acquisition	Aug 80	Sep 80	Completion delayed due to technician manpower scheduling
1.2.1.2A	Design Hot Gas Supply Duct	Jun 80	Jun 80	
1.2.1.2B	Test Hot Gas Supply Duct	Jul 80	Jul 80	
1.2.1.2	Reassemble Matrix	Aug 80	Sep 80	
1.2.1.3	Matrix Test	Sep 80		Delayed due to MTF ass'y delays
1.2.1.4	Matrix Analysis/Reporting	Nov 80		
1.2.2.1	Instrumentation/Data Acquisition	May 80	May 80	
1.2.2.2A	Replace Valve Castable	Dec 79	Dec 79	
1.2.2.2	Reassemble VTF	Feb 80	Feb 80	Addt'l mods. required to complete valve test.
1.2.2.3	Valve Test	May 80	Jun 80	
1.2.2.4	Valve Analysis/Reporting	Nov 80		
1.2.3A	Assemble Hardware	Aug 80	Aug 80	
1.2.3	Emissions Measurements	Sep 80		Completion delayed due to delayed start of Heat 203
1.2.4	Creep Testing Apparatus	Nov 80	Sep 80	
1.2.5A	Assemble Hardware	Aug 80	Aug 80	
1.2.5B	Measurements	Sep 80		
1.2.5	Characterize Effluent Air Stream	Nov 80		

Identification Number	Description	Completion Date Planned	Completion Date Actual	Comments
1.3.1A	Define Base Case Dimensions	Dec 79	Dec 79	
1.3.1	Complete Parametric Studies	Nov 80	Sep 80	
1.3.2A	Design Point Performance	Feb 80	Feb 80	
1.3.2B	Off Design Performance	Aug 80	Aug 80	
1.3.2	Complete Performance Studies	Nov 80	Sep 80	
1.3.3	Critical Component Design Concepts - Base Case	Nov 80	Sep 80	
1.3.3A	Layout Drawings	Apr 80	Apr 80	
1.3.4	Cost Estimate	Nov 80		
1.3.5	Control Concepts	Nov 80	Sep 80	
1.3.6	Matrix Support Test Facility	Nov 80		
1.3.7	Alternate Heater Systems	Nov 80		
1.3.8	Electrical Isolation	Nov 80	Sep 80	

2.0 SUMMARY

During the reporting period from July 1 through September 30, 1980, work was continued on all three tasks. The work under Task 1 included development of a method for casting a matrix support with flow passages, selection of materials for full-scale studies of an intermediate temperature air heater (ITAH), continuation of efforts on HTAH materials property determination and liaison with refractory manufacturers, preparation of a preliminary outline specification for spinel refractory bricks, preparation of "quality assurance" test methods for spinel castables, analysis of hot gas supply duct liner materials from the VTF, and continuation of efforts on thermal stress criteria.

Work under Task 2 was directed primarily toward the MTF. The MTF hot gas supply duct was tested and design modifications verified, and was reassembled for the next matrix test, Heat 203. Analysis of the test results from Valve Test 3 also continued at a low level of effort.

Under Task 3, the size/cost computer code and engineering studies planned for implementation under the Contract were completed, including studies of the relative HTAH cost with several insulation options, an assessment of the power penalty arising from HTAH valve leakage and pressurization/depressurization losses, a re-evaluation of the effects of particulate radiation in the HTAH, and several studies of individual heater performance. Work also continued on analysis of the SCAMP computer code dynamic system performance runs, study of HTAH control concepts, design efforts for a matrix support test facility, and studies of alternative heater concepts and electrical isolation needs.

3.0 DESCRIPTION OF TECHNICAL PROGRESS

3.1 Task 1 - Materials Selection, Evaluation, and Development

3.1.1 Materials Selection and Data Base

As discussed in Reference 2, a stoichiometric spinel castable with calcuim aluminate bond phase (Norton LS-812) was selected for use as the matrix support in the MTF for Heat 203. During the reporting period, a method was developed for casting this support in one piece with flow passages to match the matrix flow passages. The mold developed for this purpose is shown in Figure 1.

Wooden dowel inserts were initially used for the flow passages. This approach proved ineffective, however, because of swelling of the dowels which caused cracking of the support brick. Cardboard tubes were then chosen for the flow passage inserts. The tubes were soaked in paint to provide sufficient rigidity under the moist working conditions during casting, while remaining flexible enough not to inhibit expansion of the castable material. This approach was successful, and a support brick with minimal cracking was produced as shown in Figure 2. The support brick is shown being installed in the MTF in Figure 3.

This method could be used for producing pieces for a full-scale HTAH matrix support from a spinel castable. Significant cost savings could be realized by casting matrix support pieces rather than requiring hot pressed or sintered bricks in the complex shapes with flow passages required for a dome type matrix support. Evaluation of the performance of cast matrix support pieces in HTAH test facilities will help define whether this approach to the matrix support is viable.

Also during the reporting period, materials were selected for use in full-scale studies of alternate heater systems (see Section 3.3.7). In particular, refractory insulation schemes were selected for use in the gas and air inlet and outlet manifolds and ducts of an intermediate temperature air heater (ITAH). The materials are delineated in Table 1. The materials specified are generally more conventional than the materials proposed for the HTAH application except for the inner liner in the gas inlet manifolds and ducts. Spinel castable is proposed in this area for seed resistance. Since the materials temperatures in the ITAH are much lower than for the HTAH, development needs would be considerably reduced for a ceramic ITAH.

3.1.2 Property Determination

The objectives of this subtask are to define needs and test conditions for HTAH material property determination work carried out at FluiDyne or at other laboratories and to interpret the results in terms of the HTAH materials data base.

High temperature deformation measurements at Montana College of Mineral Science and Technology have been completed for fused cast magnesia spinel (Corhart X-317) and calcium aluminate bonded spinel castable (Norton LS-812). These materials are candidates for use in the matrix, hot liner, and matrix support in a full-scale HTAH.

The results of the measurements are shown in Figures 4 and 5. The experimental data is presented in terms of measured steady state creep rate vs. applied stress. As seen in Figure 4, when plotted in this manner, the creep rate appears to be independent of temperature; in fact, additional measurements will be required at stress levels on the order of 1-3 MPa (145-435 psi) at temperatures in the

range of 1773-1923 K (2731-3001 F) to determine temperature dependence of the creep rate.

The results do indicate that at stresses less than 1 MPa (145 psi) no measurable steady state creep was observed even at temperatures as high as 1923 K (3001 F). Mechanical stresses in all HTAH refractory materials have been shown to be less than about 1.4 MPa (200 psi) in full-scale design studies. Possible allowable creep rates are indicated in Figure 5. The Montana Tech measurements indicate that under compressive stress below about 3.25 MPa (471 psi) refractory pieces constructed from Corhart X-317 would deform less than 1% over a 75,000 hour operating life. Thus, Corhart X-317 appears to be a suitable material for use in HTAH designs from the standpoint of required mechnical loads. Results of the measurements on Norton LS-812 are still being analyzed.

Cyclic thermal stresses in the HTAH may have magnitudes many times greater than the mechanical loads (see Section 3.3.1). In order to study the interaction of a steady applied mechanical load and cyclic thermal stresses, creep measurements will be undertaken at Montana Tech in which refractory samples are loaded mechanically while being thermally cycled.

3.1.3 Liaison

Liaison with refractory manufacturers and other organizations is conducted in order to encourage development of suitable materials for use in the directly-fired HTAH. General contacts were maintained during the reporting period, but there are no new developments to report.

3.1.4 Specifications

In order to determine the level of detail required for preliminary material specifications, procurement specifications for other refractory heaters were reviewed. An outline specification was prepared for spinel brick materials which may be used for matrix bricks or hot liner bricks. This specification is included in the Appendix. The objective of work under this subtask is to prepare such specifications for the various materials required in a directly-fired HTAH. These specifications will be revised and upgraded as more information on materials requirements and material properties becomes available over the course of the heater development program.

A so-called "quality assurance" program was initiated at FluiDyne's laboratory for use initially with spinel castable materials. An outline of the procedures involved in this program is shown in Table 2. These procedures are of the type which would be followed to assure quality of material purchased for use in construction of a HTAH. The procedures will be followed as part of FluiDyne's laboratory work for two reasons, 1) to eliminate possible poor quality materials before use in the test facilities and 2) to obtain data which can be correlated to performance of spinel castable materials and eventually used in developing the material specifications.

Similar procedures will be developed for other materials over the course of the HTAH development program.

3.1.5 Materials Analyses

As discussed in Reference 1, calcium aluminate bonded spinel castable (Norton LS-812) was used in a portion of the hot gas supply duct of the VTF. This material degraded badly, in contrast to excellent performance as a matrix hot liner in the MTF. Analysis of a sample of the degraded castable was obtained from the manufacturer during the reporting period. The manufacturer's report is summarized in the following:

> "The evaluation from a ceramic point of view evolves around the material's microstructure and the phase composition changes occurring at the reacting surface. X-ray diffraction and petrographic microscopy of the cross sections were employed in this determination.
>
> The microstructure of the sample submitted is a high density, low porosity spinel refractory. Porosity and spinel grain size do not appear to have changed in the unreacted area (see Figure 6) and at the reacted zone (see Figure 7.) Likewise, the amount of glassy phase between the grains does not appear to change between the unreacted zone and the hot face of the specimen.
>
> The phase composition of the hot face indicated the presence of major spinel, moderate amounts of forsterite ($2MgO.SiO_2$) and enstatite ($MgO.SiO_2$) and trace amounts of alumina. The unreacted area of the refractory had major spinel and minor amounts of alumina present.
>
> The mode of failure was characterized by attrition of the refractory during 55 hours of exposure as evidenced by the increase in inner diameter at the combustion zone.

The failure mode thus appears to be due to the reaction of silica in the coal ash with the refractory lining in the combustion chamber. This reaction is indicated by the presence of enstatite ($MgSiO_3$) and forsterite (Mg_2SiO_4) in the hot face sample. Since enstatite melts well below the temperature in the combustion chamber, liquid (glass) would be expected to be found at the hot face. Figure 7, a photomicrograph taken at the hot face, and Figure 6, taken in the unreacted refractory about 1.5 cm in the hot face, show equal amounts of glass in both zones. The reason glass is not observed is that when it forms at the spinel grain boundaries and refractory surface, it is swept from the refractory face by the turbulence generated in the combustion chamber. Therefore, there was a constant attrition of the exposed refractory during the test. This reaction is more rapid where a smaller grain size is present at the hot face (Figure 8).

The reaction that occurs at the hot face can best be illustrated by the ternary phase diagram (Figure 9) of MgO-Al_2O_3-SiO_2. Assuming the overall composition of the refractory is at the spinel composition on the MgO-Al_2O_3 binary juncture at the base line, the composition moves toward the SiO_2 apex. The bulk composition at the hot face becomes more silica rich and spinel reacts with the liquid at 1800 C about half way through the spinel stability field to form corundum, forsterite and liquid. With further melting, the more siliceous enstatite is stabilized. It appears that this is the reaction occurring along the hot face of the refractory.

The reaction is much more complex than this as there are other components present such as CaO, Fe_2O_3, K_2O, etc., which would depress the melting point further. The above mechanism is felt to be the principal reaction leading to erosion and eventual failure of the refractory."

Thus it appears that an ash reaction is the primary cause of failure of the spinel castable material. It appears that in the region of the hot gas supply duct where the seed has not yet vaporized the spinel material does not resist the ash corrosion whereas in other test regions, including potassium vapor, this material has performed well. As discussed in References 1 and 2, and in Section 3.2.1, re-bonded fused grain magnesia chrome (Corhart RFG) has performed well in the regions of the hot gas supply ducts near the combustors of the MTF and VTF.

3.1.6 Thermal Stress Criteria

Preliminary results of the thermal cycling test work at Montana College of Mineral Science and Technology have been obtained. Lamé constants, which are used to define the mechanical properties of materials, have been measured ultrasonically in cylinders of fused cast magnesia-spinel (Corhart X-317) before and after exposure in the thermal cycling test apparatus. The data is being evaluated and will be presented in the next quarterly progress report.

3.2 Task 2 - Operability, Performance, and Materials Testing

3.2.1 Matrix Test Facility (MTF)

During the reporting period, the MTF hot gas supply duct was tested to confirm that its redesign had corrected earlier experimental difficulties, and reassembly of the remainder of the MTF was completed.

The test of the MTF hot gas supply duct was run during the week of July 21. The conditions for the test were selected to match the operating conditions during the gas phase for Heat 203, the next test of the MTF which will be run during the next quarterly reporting period. The duct was tested for 60 hours of continuous operation with a mass flow rate of 0.13 kg/sec (1000 lbm/hr) and a duct exit gas temperature of approximately 1978 (3100 F). The solids injection rate was controlled to produce a gas composition including 1% by weight potassium (2.3% potassium sulfate) and 0.1% by weight Montana Rosebud ash.

The test duration of 60 hours at test conditions was selected so that the test could be completed in one work week, including time required to reach operating conditions and to shut down after completing the test, while still having a long enough duration to assess the duct liner materials performance. The test duration represented 30% of the time that the hot gas supply duct will be operated with seed/ash injection during the upcoming 300 hour matrix test (Heat 203).

The results of the test indicate that the redesigned hot gas supply duct will not cause a recurrence of the earlier experimental problems over the course of running Heat 203. The duct walls remained intact, with no significant degradation of the magnesia chrome (Corhart RFG) material. In addition, no significant amount of seed/ash material was deposited in the duct. This result dispels a possible concern about disentrainment of the injected particles due to low velocity in the duct, the diameter of which had been increased to prevent impingement of the expanding flame jet on the duct walls.

Reassembly of the MTF and installation of temperature and pressure instrumentation was completed. The matrix was assembled using the materials delineated in the previous quarterly progress report with one exception. An experimental material under development by the Carborundum Company was not received from the manufacturer and thus, was not used at the top of the matrix. The uppermost 5% of the 5.2 m (17 ft) cored brick matrix was constructed from fused cast chromia (Carborundum Monofrax E). The next 45% of the matrix was constructed from magnesia-spinel (Corhart X-317) bricks which had previously been used in the matrix during Heat 201, which had a duration of 420 hours, and Heat 202, which had a duration of 750 hours. Pristine magnesia-spinel was used for the next 40% of the matrix. The lowermost 10% of the matrrix was constructed from sintered spinel bricks (Norton SX-471). The matrix support was made from calcium aluminate bonded spinel castable (Norton LS-812) as described in Section 3.1.1.

The objectives of the test are as follows:

1. operation of the MTF for 300 hours without accumulation of deposits in the matrix flow passages,

2. accumulation of testing time on the previously used magnesia-spinel bricks,

3. evaluation of the fused cast chromia material for use at the top of the matrix,

4. evaluation of the sintered spinel material for use at the bottom of the matrix,

5. evaluation of the castable matrix support,

6. emissions and chemical composition measurements as discussed in Sections 3.2.3 and 3.2.5, and

7. evaluation of several high temperature instruments for use as diagnostic and/or control instrumentation in future test work and full-scale HTAH systems.

Details of the test and discussion of the results will be presented in the next technical progress report.

3.2.2 Valve Test Facility (VTF)

Efforts under this subtask were limited to compilation of data collected during Valve Test 3. Some information regarding the temperature data from the castable refractory insulation in the test valve remains to be assembled from the raw data collected during this test. A summary of the test data will be presented in the next technical progress report.

3.2.3 Emissions Measurements

The necessary sampling hardware was assembled and the sampling requirements were specified during the operating period. The emissions measurements will be conducted during Heat 203 in the MTF. Gas samples will be extracted from the MTF with a water cooled probe and analyzed for O_2, CO, CO_2, and NO_x. Measurements will be made in the gas entering the top of the matrix and leaving the bottom of the matrix. NO_x levels will be compared to determine whether the matrix acts to catalytically reduce the NO_x level.

In addition to the gas sampling, particulate concentration measurements will be made downstream of the baghouse.

3.2.4 Creep Testing Apparatus

Design of a dilatometer for making creep measurements in the HTAH service environment was completed during the reporting period. Construction and testing of the dilatometer have not been authorized under this Contract but are anticipated at some future date.

In order to be able to design high temperature air heaters for MHD power plants, creep data will be needed for the various matrix, hot liner, and insulation materials at the service temperatures. At present, creep data for most refractories in unavailable at the high temperatures required. High temperature creep measurements are underway at Montana Tech for a number of HTAH candidate materials. Such measurements can only be made in heated air, however. The question of how the seed/ash laden MHD gas affects the creep behavior of refractories can be addressed in such tests only by making measurements on samples which have been exposed to the HTAH service environment. In order to confirm that this procedure correctly predicts the results of seed/ash exposure on materials under load, it will be important to make some creep tests in the HTAH service environment. For this reason, a creep test apparatus was designed which can be used to test materials under load while being subjected to the simulated HTAH service environment of the MTF.

The dilatometer design is shown in Figure 10. A brief description is given in the following.

Adaptation To Matrix Test Facility

The dilatometer has been designed for installation in the hot gas duct of the Matrix Test Facility. The dilatometer duct I.D. is 0.15 m (6 in.). End flanges are provided to mate a nominal 0.76 m (30 in.) diameter pipe. This adaptation is to allow creep tests to be performed as piggy-back tests during other MTF tests, thus reducing the costs of the creep tests. The dilatometer may be mounted as a part of the MTF hot gas duct through which the entire hot gas flow is passed. However, erosion due to liquid ash particles may be a problem in this configuration. Thus, the dilatometer will most likely be mounted as a bypass leg or as a right-angle extension of the MTF hot gas supply when creep tests are performed.

Horizontal Configuration

The dilatometer is designed with the hot gas duct oriented horizontally and with the refractory test sample held transverse to the gas flow and also in a horizontal position. This configuration will keep the sample and the measurement components of the dilatometer from being exposed to liquid seed and/or slag which may be present in the bottom of the hot gas duct.

Measurement Symmetry

The function of the dilatometet is to measure the change in length of a sample subjected to a compressive load. The load is also measured. Perhaps the most unique feature of the design is measurement symmetry, i.e., all components involved in the measurement of the change in length of the sample are identical at both ends of the sample. They are geometrically identical as well as being similar in terms of their thermal environment. This symmetry should greatly reduce the need for

complex calibrations prevalent in most existing dilatometers where at least one of the rods translating the displacement of the sample to a transducer is located in the test gas stream or the test cavity of a furnace.

Access To Sample and Viewport

The upper portion of the dilatometer duct is a removable section for access to the test sample. This section of the duct also contains an air-cooled viewport for observing the test sample throughout the test.

Cooling Systems

The design has two primary cooling systems, one with air cooling and one with water cooling.

The air cooling system has two inlets located near each of the displacement transducers. The purpose of the air cooling is two-fold. First, the air cooling keeps the transducers cool and, secondly, it provides air to purge the gaps around the measurement rods and the rams to prevent contamination by seed or ash in the hot gas stream. The cooling air is discharged to the hot gas stream.

The water cooling system cools the jacket of the dilatometer duct including the access cover and the duct support frame. The water cooling on the duct minimizes the amount of duct insulation required and reduces thermal expansion on all metal parts. The water cooling in the support frame reduces thermal expansion in that component. The two water cooling systems (duct including cover and support frame) may be supplied in series at a flow rate of .015 m^3/hr (4 GPH). The estimated water temperature rise at this flow rate is less than 5.6 K (10 F).

Measurement Range and Samples

The dilatometer was designed for the capacity to make creep measurements at stress levels up to the maximum encountered in full-scale MHD HTAH studies. The maximum stress levels reached in various heater concepts was approximately 1 MPa (150 psi). The design can apply up to 890 N (200 lbs) on a refractory sample having any diameter up to a maximum of 38 mm (1.5 in.) along the centerline with less than 0.08 mm (0.003 in.) displacement of the centerline from rest. Each transducer core has a translation range of $\pm$ 5.08 mm (0.200 in.). The transducers are Schaevitz Type E-200 whose maximum operating temperature is 367 K (200 F). The load cell is a standard 1.8 kN (400 lb) FluiDyne load cell, Drawing No. 020342A.

Consumables

In the event of a fracture of a sample, it is probable that the sapphire measurement rods and the ram end caps will be damaged or broken. These same components could also be damaged by chemical attack by the hot gas stream. These consumables would cost up to $1000 for a complete test set based on a single order price. Quantity orders (5 to 10 sets) could reduce the price by nearly 50%. These prices are based on sapphire measurement rods approximately 152 mm (6 in.) long. The design provides for the shortening of these rods by replacing the cool end with interchangeable metal extensions.

3.2.5 Effluent Air Stream

The test procedure to be used for characterization of the effluent air stream has been specified. The actual measurement will be made during Heat 203 of the MTF.

The interest in the measurements lies in determining the level of potassium which is picked up by the air stream as it passes through the cored brick matrix. This information bears on the electrical isolation problem in an HTAH.

Toward this end, samples of the air leaving the top of the matrix will be extracted with a water cooled probe and bubbled through a distilled water blank. The probe will then be washed, and the blank and probe wash will be analyzed for potassium content. This procedure will be followed for measurements over an entire air phase, over halves of an air phase, and over thirds of an air phase, in order to obtain information on the total amount of potassium carryover and on the time history of the potassium carryover.

3.3 Task 3 - Full-Scale Design Concepts

3.3.1 Size/Cost Analysis and Parametric Studies

In order to assist in identifying HTAH development needs and defining goals for the HTAH development program, work under this subtask involves use of the size/cost and other computer codes and engineering studies of the impact of particular HTAH systems or components. During the reporting period, several modifications to the size/cost computer code were completed, and size/cost analysis of the "FY 80 case" (summarized in Table 3) was completed. Engineering Studies were conducted of the effect of HTAH valve leakage and pressurization/depressurization losses on the overall MHD plant and of the effect of particulate matter in the MHD gas stream on radiation heat loss in the HTAH system. Studies of the performance of individual heaters in the HTAH were also made using the STRHEX computer code.

Size/Cost Studies

Modifications to the size/cost code included corrections to and upgrading of the refractory intersection cost model for intersections of ducts and manifolds, incorporation of a model for the heater vessel plenums as conceived in the FY 80 HTAH system layout, inclusion of an option for examining either constant-area or decreasing-area submanifolds for connecting groups of individual heaters, and allowing the heat flux through the insulation to vary at different locations in the HTAH system (i.e., in the manifolds, ducts, heater vessels, etc.). Once these modifications were completed and checked, size/cost code analysis of the FY 80 HTAH was completed.

Comparison of the cost of an HTAH having the performance and size requirements defined for the FY 80 case, but with various insulation schemes, are shown in Table 4. These comparisons demonstrate the importance of the insulation scheme to the total HTAH cost and the need for development of insulation materials to achieve the lowest potential cost.

The first column, lowest risk brick, represents an insulation system in which all material layers are constructed of bricks having ample thicknesses for structural integrity. In addition, high density, seed resistant materials are specified for use in all areas where the temperature is greater than 1289 K (1860 F) as an assurance against attack by potassium containing vapors. This system therefore has the lowest risk of failure and correspondingly, the highest cost of the systems considered.

The second column in Table 4 represents a system in which the brick thicknesses are reduced and the potassium vapor problem is not considered beyond the so-called "hot liner" surrounding the heat storage matrix. A large cost reduction is realized, along with a corresponding greater risk due to the uncertainty of structural integrity and the possibility of alkali vapor corrosion.

An even greater cost reduction is seen in the third system, in which monolithic or castable insulating refractories are used. This insulation system also has greater risk than the most conservative brick scheme due to questions of structural integrity, anchoring requirements, and alkali corrosion resistance. A scheme utilizing brick and castable combinations, as shown in the fourth column, also represents a cost reduction over the lowest risk brick system, although not as great as for the higher risk brick or monolithic insulation schemes.

The final column in Table 4 represents the insulation materials selection reported in Reference 1, in which four layers of insulation were proposed, including an insulating spinel brick and a high strength insulation brick capable of withstanding the temperature and alkali corrosion resistance requirements of the HTAH. Again, a significant cost reduction is seen over the lowest risk brick insulation scheme, but not as great as for the other reduced cost schemes.

These cost comparisons show the importance to the overall HTAH development program of developing insulation materials and construction techniques which will allow the use of improved insulation schemes and result in reduced cost of HTAH. Thus, a primary goal of the work under Task 1, Materials Selection, Development and Evaluation is to select materials

for testing and property determination which will meet the criteria posed by the most cost-effective schemes illustrated in Table 4. Testing and evaluation of castable materials and high strength insulating brick have the highest priority for insulation materials. It must be emphasized however, that even the lowest risk brick insulation scheme would require subscale and large scale testing under HTAH conditions to verify performance.

Another cost comparison is shown in Table 5, in which reducing the size of the HTAH system manifolds is considered as a potential cost reducing method. The magnitude of cost reduction is on the same order as that obtained by using the four layer insulation scheme. In the case of manifold size reduction, the benefits of decreased cost must be balanced against effects on total system performance (see Section 3.2.2) and possible duct erosion due to higher velocity.

Effect of Leakage and Pressurization/Depressurization Losses

The effects of mass loss due to valve leakage and pressurization/depressurization losses on the overall MHD plant was studied. Valve leakage results in a loss of pressurized combustion air; this leakage flow bypasses the combustor, channel, and radiant boiler and passes directly to the components downstream of the HTAH. Pressurized air is also lost to the downstream components when the individual heaters are depressurized after each air phase by discharging air to the gas outlet manifolds. In addition, a residual inventory of low pressure channel exhaust gas is mixed with the pressurized combustion air after each gas phase as the heater is pressurized.

The effect of this overall mass loss on the overall plant is minimal. No penalty is incurred in the downstream components; the air mass lost from the HTAH can be compensated for by reducing the secondary combustion air which is added upstream of the bottoming plant. Since combustion air to the MHD combustor is lost, however, additional pressurized air must be supplied to the HTAH in order to maintain the required total channel flow and temperature. This additional air imposes a penalty in the form of power required to compress the air which will be lost by leakage and pressurization/ depressurization.

The additional compressor power required may be estimated by the following equation.

$$P \simeq \frac{\dot{m}\ Cp\ T_1}{\eta_m\ \eta_c} - \left[\left(\frac{P_2}{P_1} \right)^{(\gamma-1)/\gamma} - 1 \right]$$

where $\dot{m}$ is the additional mass flow required to compensate for valve leakage and pressurization/ depressurization losses

Cp is the specific heat of air

T_1 is the compressor inlet temperature

η_c is the compressor efficiency

η_m is the efficiency of a compressor drive motor

P_2/P_1 is the pressure ratio

γ is the ratio of specific heats for air

The following assumed values were used:

$P_2/P_1 = 9$

$T_1 = 288$ K (519 R, 59 F)

$\eta_c = 0.87$ (no intercooling)

$\eta_m = 0.98$

A small power recovery is realized by the bottoming plant since the compressor outlet temperature will be greater than the stack temperature of the bottoming plant. This recovered power can be estimated by:

$$P_R \simeq \dot{m}\, C_p (T_2 - T_{stack})\, \eta_\beta$$

Where T_2 is the compressor outlet temperature

T_{stack} is the bottoming plant stack temp.

η_β is the bottoming plant conversion efficiency

The following assumed values were used:

$T_2 = 578$ K (1040 R, 580 F)

$T_{stack} = 422$ K (760 R, 300 F)

$\eta_\beta = 0.33$

The net additional power required to compensate for valve leakage and pressurization/depressurization losses is thus given by

$$P_{net} = P - P_R$$

The effect of this additional power requirement on the overall plant efficiency is shown in Figure 11 for a 1000 MW_e power plant. Calculations were made for two cases, a plant having an overall efficiency of 45% and a plant having an overall

efficiency of 50% (computed without accounting for the additional power required to compensate for mass loss due to valve leakage and pressurization/depressurization losses).

The loss in efficiency is plotted vs. the time averaged mass loss in Figure 11. Three values of the mass loss are indicated. First, a value is shown which represents a calculation of the net mass exchange due to pressurization/ depressurization for the "FY 80" case example HTAH discussed in Reference 1. The second value adds to this pressurization/ depressurization loss a total valve leakage mass loss estimated on the basis of results of valve tests reported in Reference 2. The third value includes total valve leakage as computed by the size/cost computer code for the FY 80 case in addition to the pressurization/depressurization loss. It should be noted that these calculations of mass loss are all based on the FY 80 example HTAH which has 30 individual heaters. A HTAH having a smaller number of heaters would have a smaller total mass loss.

The effect on total plant efficiency is seen to be quite small. For example a plant having an efficiency of 50.00% when disregarding mass loss in the HTAH has an efficiency of 49.96% when the additional power requirement due to mass loss is accounted for, based on estimates from the valve testing results. Even when the more pessimistic size/cost computer code calculations are used, the efficiency is reduced to only 49.91%. Corresponding reduced efficiencies for a plant having 45.00% efficiency with no mass loss are 44.96% and 44.93%. The use of a directly-fired HTAH can raise the overall plant efficiency by 5 or more percentage points over a system with oxygen enrichment. Thus, efficiency reductions on the order of 0.04% to 0.09% are insignificant when compared to the overall efficiency advantage realized through use of the directly-fired HTAH.

Effect of Particulate Radiation

Due to the recent availability of material on particle size and distribution and heat transfer in the MHD channel, diffuser, and radiant boiler (Refs. 3-5), the radiative heat exchange model used in the size/cost computer code and other HTAH computational models was reviewed. The contribution to the total heat transfer due to radiation exchange between particulate matter in the gas stream and duct or flow passage walls has been estimated in previous work from assumed particulate concentrations and size distributions. This contribution has been recalculated using information given in References 3-5 for use in future full-scale studies work.

The results of these calculations are shown in Figure 12. As can be seen in this figure, the magnitude of particle radiation is fairly small for small passage diameters, such as the heat exchange matrix flow passages. The magnitude of the particle radiation term increases toward a maximum value as the passage diameter increases, for example in the large manifolds carrying the radiant boiler exhaust gas to the HTAH. Incorporation of the improved particulate radiation term as shown in Figure 12 will improve the HTAH simulation in future full-scale studies.

Individual Heater Performance

As discussed in Reference 2, the STRHEX computer code was upgraded during the previous quarterly reporting period to provide the capability to examine several particular concerns of the HTAH development program. The program was used during this reporting period to study the effect of individual heater droop on thermal stresses and the effect of heater vessel heat loss on the radial temperature profile in the heat storage matrix. The calculations were made for the conditions defined for an ideal heater in the FY 80 example HTAH as defined in Reference 1.

Calculations of the thermal stress at the inner surfaces of the heater matrix flow passages are shown in Figure 13. The cored brick material is stressed in tension during the air phase and in compression during the gas phase. The most severe thermal stress occurs at the bottom of the matrix during the first 40% of the air phase. This condition results from the need to raise the bottom of matrix solid temperature to a level of 1400 K (2060 F), at the end of the gas phase to promote drainage of seed/slag from the matrix flow passages. The low temperature, 922 K (1200 F), air which is introduced at the bottom of the matrix then results in a very high stress levels, which decay as the solid temperature decreases. The thermal stress levels are much lower at the middle and top of the matrix.

This result emphasizes the need for matrix materials which are resistant to cyclic thermal stresses, particularly in the bottom region of the matrix where the variation in stress level over the course of a heater cycle is very large.

Calculations of the radial temperature profile across the cored brick matrix at the end of the gas phase are shown in Figure 14. The three curves were computed using different models for the thermal resistance of the flow passages; models 1 and 2 represent upper and lower limits on the thermal resistance of the flow passages while model 3 falls between these extreme values.

As can be seen from these profiles, for the FY 80 example HTAH conditions, a temperature variation on the order of 19 K (35 F) can exist in the matrix. This is especially important to consider in HTAH design at the bottom of the matrix, where a minimum temperature of 1400 K (2060 F) is specified at the end of the gas phase for effective seed/slag drainage. To assure that the seed/slag material drains effectively at the outer edges of the matrix, a temperature as high as 1419 K (2095 F) may be required in the center of the matrix.

3.3.2 Dynamic System Performance Simulation (SCAMP)

No additional runs of the SCAMP code were made during the reporting period; efforts were confined to analysis of the results from the four SCAMP runs made previously. These runs were made for the FY 80 example HTAH layout having 30 small diameter heaters for a 1000 MW_e plant (see Ref. 1). A brief summary of results is given in the following for the SCAMP runs denoted as:

1. Large manifolds - gas and air inlet and outlet manifolds sized to allow a velocity no greater than 30 m/sec (100 ft/sec); 2000 sec gas phase and 800 sec air phase for each individual heater.

2. Small manifolds - manifolds reduced in diameter by $\sqrt{2}$ to give maximum velocity of 60 m/sec (200 ft/sec); 2000 sec gas phase and 800 sec air phase for each individual heater.

3. Small manifolds with control - air and gas phase durations fixed individually for individual heaters to control maximum bottom of matrix solid temperature (see Section 3.3.5).

The results of these runs are summarized in Table 6, and the outlet air temperature over the total 30 heater cycle for each run is shown in Figures 15-17.

The air outlet temperature variation with large manifolds is 24 K (44 F) and the gas outlet temperature variation is 16 K (29 F). With small manifolds, the air outlet temperature variation increases to 50 K (90 F) and the gas outlet temperature variation increased to 31 K (56 F). Thus the reduction in manifold size, which reduces the HTAH cost by 9% (Table 5), doubles the air and gas outlet temperature variations.

The increase in outlet temperature variation with decrease in manifold size arises from the resulting degree of variation in flow through the individual heaters in the system. Comparing Figures 15 and 16, it is evident that the short term ($\sim$ 1.5 minute) variations in air outlet temperature, which arise from the temperature droop in the individual heaters, are essentially unchanged in the small manifold case. However, a longer term ($\sim$ 10 min.) variation in outlet temperatures also exists. This longer term variation is due to the fact that the location of each individual heater relative to the air and gas manifolds affects the amount of flow it receives, since the pressure loss in the manifolds is not insignificant relative to the pressure loss in the heater flow passages. Heater-to-heater differences in the flow rate produce heater-to-heater differences in performance; thus different heaters produce different <u>levels</u> of air outlet temperature even through the <u>droop</u> in temperature remains nearly the same. When the manifold size is decreased, the pressure loss in the manifolds becomes even more significant and differences in flow rate are increased. The longer term variations in system outlet temperature are then increased.

In order to effectively drain seed/slag from the heaters during normal operation of the HTAH, the bottom of matrix solid temperatures must exceed the melting point of seed (1342 K or 1956 F for potassium sulfate) for a sufficient period of time during each gas phase. In order to assure that this condition is realized, 1400 K (2060 F) has been selected for the criterion which the maximum bottom of matrix temperature of each individual heater should meet or exceed. Neither the large nor small manifold system, operating with all heater cycles having the same gas and air phase durations, meet this criterion (Table 6, third column). Some individual heaters have maximum bottom of matrix temperatures as low as 1336 K (1944 F) for the large manifold case

and 1279 K (1843 F) for the small manifold case. This is because of the variation in the flow rates, and thus heater performance, due to location of the individual heaters relative to the manifolds as discussed above.

For this reason, a control system was implemented in the SCAMP model to determine whether the bottom of matrix temperature criterion could be achieved. The control concept was to allow each individual heater to operate with different durations of gas and air phases to compensate for the differences in flow (see Section 3.3.5). As seen in Table 6, when this concept was used with the SCAMP code for the small manifold HTAH, the maximum bottom of matrix temperature criterion for all heaters was nearly achieved. A new choice of phase durations for the individual heaters could have been made in order to improve the bottom of matrix temperatures further, but since the capability of the control concept had been demonstrated, another SCAMP run was not made in consideration of budget constraints.

The air outlet temperature for the small manifold HTAH with control system is shown in Figure 17. The total variation in air outlet temperature is the same as for the small manifold case without control, although the form of the outlet temperature over time is different. This result demonstrates the capability to operate a HTAH in such a manner as to control a particular parameter, in this case as required for heater operability, while maintaining the overall HTAH performance.

3.3.3 System Layouts

The objective of this subtask is to prepare HTAH system layouts for the purpose of integrating individual component modeling or design studies. The level of effort for the layouts will be consistent with that needed to identify development needs.

No effort was expended under this subtask during the reporting period.

3.3.4 Cost Estimates

The objective of this subtask is to prepare a cost estimate for the FY 80 case based on the system layouts as established under Section 3.3.3. The intent of the cost estimate is to provide a check of the ability of the size/cost computer code to produce realistic cost estimates to aid in identifying areas of the HTAH where significant cost savings can be achieved.

Minimal effort was expended during the reporting period; cost estimating procedures were reviewed in conjunction with revisions to the size/cost code (see Section 3.3.1).

3.3.5 Control Systems

The objective of this subtask is to screen and define HTAH control needs and systems. Performance data from dynamic modeling with the SCAMP computer code is used for this purpose.

A control concept was identified in Reference 2, and a SCAMP run using this control concept was discussed in Reference 2 and in Section 3.3.2. The concept was developed from the need to increase the maximum bottom of matrix solid temperature for certain of the heaters, as noted in the other SCAMP runs, in order to achieve the criterion of 1400 K (2060 F) discussed earlier to insure effective seed/slag drainage from the flow passages.

The concept was to allow those individual heaters which did not achieve the temperature criterion to operate with a lengthened gas phase and a shortened air phase, maintaining the same total heater cycle time so that the heater sequence is not affected.

The method used to select the changes in the gas and air phase durations was as follows. Several runs were made with the STRHEX code, modeling an individual heater in the FY 80 example HTAH. The phase durations were systematically varied to produce the curve shown in Figure 18, which indicates the amount that the phase duration should be modified to achieve a corresponding change in maximum bottom of matrix temperature. The results showed that the temperature would vary as a linear function of the change in phase duration. The durations of the air and gas phase for several heaters were then altered to achieve the desired result. Secondary effects due to changes in phase duration of other heaters in the system were ignored for the first attempt at implementing the control concept. This resulted in the previously mentioned deviation from the ideal result which was sought.

This control concept could be readily used in an actual HTAH system. Sensing of a temperature which is too low or a pressure drop which is too high would result in an adjustment of the phase times by the HTAH controller. Study of the system response with regard to those parameters which affect the overall MHD plant performance will be required in order to evaluate the possible use of this or other control concepts. Analysis of the SCAMP data from the runs made to date and of future SCAMP data will be directed toward this objective.

3.3.6 Matrix Support Test Facility

The objective of this subtask is to identify the requirements which must be met by a future test facility for testing matrix support concepts at nearly full-scale.

During the reporting period, data concerning the matrix support requirements for the FY 80 example HTAH were reviewed and an initial concept for the matrix support test facility was developed. Definition of the test facility, including preparation of engineering drawings, will be completed during the next quarterly reporting period.

3.3.7 Alternative Heater Systems

Three alternate directly-fired heater concepts are being considered. The first is a cored brick heater in which the reheat gas flows vertically upward. This concept results in a temperature gradient which is in the same direction as the gravitational field, thus promoting seed/slag drainage. Expected constraints on refractory creep of the matrix support will limit the inlet gas temperature to about 1589 K (2400 F); the achievable air preheat will thus be somewhat lower than for the basic HTAH concept.

The second and third concepts involve so-called "Intermediate Temperature Air Heaters" (ITAH) in which the radiant boiler outlet temperature is reduced to a level of approximately 1311 K (1900 F) upstream of the heater. In this system any seed/slag material present in the reheat gas will be present in a "dry" solid form. This avoids problems related to sticky ash and to seed which undergoes phase changes from vapor to liquid to solid. Two versions of the ITAH will be considered, a cored brick type heater and a pebble bed type heater.

An insulation concept has been selected for the cored brick ITAH as presented in Section 3.1.1. Modifications to the size/cost computer code to allow use of the selected insulation materials and criteria are nearly complete. Insulation selection and implementation in the size/cost code for all three concepts will be completed and final conceptual size/cost runs made during the next quarterly reporting period.

3.3.8 Electrical Isolation

The objective of work in this area is to identify development needs concerning electrical isolation of the HTAH from the MHD combustor. This activity is conducted at a low level of effort under the scope of the contract.

During the reporting period, electrical conductivity of air at various temperatures and with various degrees of potassium contamination was determined with assistance from Dr. R.H. Eustis at Stanford University. The results are shown in Table 7. Test data on the amount of potassium carried over to the effluent air stream (Section 3.2.5) will be used in conjunction with these calculations to estimate the severity of electrical conduction through the air stream.

Calculations of the electrical conductivity of typical hot liner refractories at air outlet manifold temperatures were also made. These calculations showed that the innermost refractory materials, even without any seed deposits, are conductive enough to present an isolation problem if the isolation section is very short. Thus, a gap in the refractory insulation will probably be required for electrical isolation.

4.0 CONCLUSIONS

A potential cost-saving method for construction of a full-scale matrix support was identified through selection of a castable material for the matrix support in the MTF and development of a technique for installing it. Size/cost computer code studies have shown that the selection of an insulation scheme for a full-scale HTAH is a major factor in determining HTAH cost. A four-layer insulation scheme selected for full-scale studies was shown to result in a cost lower than the lowest risk insulation scheme but greater than schemes using castable insulation materials.

Measurements at Montana Tech have shown that fused cast magnesia-spinel (Corhart X-317) has sufficient creep resistance to withstand HTAH design loads with no significant deformation.

Design of a dilatometer for making measurements of refractory creep in the directly-fired HTAH service environment was completed. Construction and testing of this device at a future time in the HTAH development program will allow confirmation of creep information inferred from the conventional creep tests (at Montana Tech) of pristine material samples and samples which have been exposed to the HTAH environment.

Mass loss in a HTAH due to valve leakage and pressurization/depressurization losses was shown to result in a reduction of MHD plant efficiency of less than 0.1%. When compared with the gain in efficiency resulting from use of a HTAH, this penalty is negligible.

Analysis of HTAH system and individual heater performance had demonstrated the capability to control HTAH performance parameters using a concept under which the lengths of time that individual heaters are on gas and air phases are varied as required while a constant total cycle time is maintained.

REFERENCES

1. FluiDyne Engineering Corp., MHD Air Heater Development Technology, Progress Report for period November 26, 1979 - March 31, 1980. Prepared for DOE under Contract #DE-AC01-80ET15602, May 1980.

2. FluiDyne Engineering Corp. MHD Air Heater Development Technology Progress Report for period April 1, 1980 - June 30, 1980. Prepared for DOE under Contact #DE-AC01-80ET15602, July 1980.

3. Ahluwalia, R.K., and Im, K.H., "Heat Transfer Scaling Laws for MHD Channels and Diffuser," Proceedings of Seventh International Conference on MHD Electrical Power Generation, Massachusetts Institute of Technology, Cambridge, Massachusetts, June 16-20 1980, pp. 187-194.

4. Im, K.H. and Ahluwalia, R.K. "Heat Transfer Scaling Laws for MHD Radiant Boilers," Proceedings of Seventh International Conference on MHD Electrical Power Generation, Massachusetts Institute of Technology, Cambridge, Massachusetts, June 16-20 1980, pp. 329-336.

5. Ariesson, P.C., Eustis, R.H., and Self, S.A., Measurements of the Size and Concentration of Ash Droplets in Coal-fired MHD Plasmas," Proceedings of Seventh International Conference on MHD Electrical Power Generation, Massachusetts Institute of Technology, Cambridge, Massachusetts, June 16-20 1980, pp. 807-814.

TABLES

TABLE 1

Insulation Schemes for ITAH
(Based on Plane Wall)

Interface Temperature K (F)	Material	Thickness m	Thickness (in.)	
1311 (1900)				
	Norton LS-812 (Spinel Castable)	0.15	(6)	Gas Inlet Manifold/Ducts $Q = 918\ W/m^2$ (291 Btu/hr-ft^2)
1230 (1754)				
	Sauerisen No. 72 (acid resistant cement)	0.30	(12)	
367 (200)				
	Shell			
1311 (1900)				
	A.P. Green Lo Abrade (Castable)	0.15	(6)	Air Outlet Manifolds/Ducts $Q = 931\ W/m^2$ (295 Btu/hr-ft^2)
1106 (1530)				
	A.P. Green Castable No. 20 (Fireclay)	0.23	(9)	
367 (200)				
	Shell			
755 (900)				
	Sauereisen No. 72 (acid resistant cement)	0.13	(5)	Air Inlet and Gas Outlet Manifolds/Ducts $Q = 994\ W/m^2$ (315 Btu/hr-ft^2)
367 (200)				
	Shell			

TABLE 2

Test Program
For Spinel Castables

Item	Type of Test	Possible Diagnostic Uses	ASTM No.
1.	Sieve analysis	Affects bulk density, strength, dimensional changes after firing. Gross differences may indicate improper cement: aggregate ratio	C 371
2.	Water used to cast (i.e., to attain proper ball-in-hand consistency)	Influenced by amount and quality of cement and, to a lesser extent, by aggregate size distribution. Also influenced by care and skill used to prepare test pieces.	C 860
3.	Linear dimensional change after drying	Relatively insensitive to minor quality variations.	C 134
4.	Bulk density of test bars after drying	Relatively insensitive to minor quality variations.	C 134
5.	Strength after drying (preferrably M.Ø.R.)	Affected by amount and quality of cement in mix and, to lesser extent, aggregate size distribution.	C 133
6.	Linear dimensional change after firing to 2900°F w/5 hour soak	Affected by factors listed under Item 5 plus chemical purity.	C 134
7.	Strength (preferably M.Ø.R.) after firing to 2900°F w/5 hour soak	Same as Item No. 6, but M.Ø.R. test is more sensitive to quality changes	C 133
8.	Chemical analysis (CaO, MgO, Fe_2O_3, SiO_2, and alkalis)	Very important influence on performance at the highest temperature	Various

TABLE 3

DESCRIPTION OF EXAMPLE DIRECTLY-FIRED HTAH FOR 1000 MW_e PLANT (FY 80 CASE)

Item	MHD Gas	Air	Units
Flow in	836 (1844)	683 (1506)	kg/sec (lbm/sec)
Flow Out	849 (1872)	670 (1478)	kg/sec (lbm/sec)
T_{in}	1978 (3100)	919 (1200)	K (F)
T_{out}	1326 (1926)	1788 (2748)	K (F)
P	869 (126)	108 (15.6)	kPa (psi)
ΔP	4.5 (0.65)	17.2 (2.5)	kPa (psid)
Vessels	20	8	Heaters
Flow Duration	2000	800	Seconds
Heat Duty	706 (6.7×10^5)		MW (Btu/sec)
Bed Diamater	4.3 (14)		m (ft)
Bed Height	6.7 (22)		m (ft)
Thermal Stress	25.5 (3700)		MPa (psi)
Hole Size/Web	25/14 (1.0/0.55)		mm (inches)
P/DP Units	2		Vessels
Inlet Valve Diameter	2.2 (86)	0.8 (31)	m (inches)
Outlet Valve Diameter	1.8 (72)	1.1 (42)	m (inches)
Heat Loss	6		Percent

TABLE 4

HTAH Cost Comparisons for
Various Insulation Schemes

HTAH Component	Insulation Scheme: Lowest Risk Brick	Higher Risk Brick	Monolithic	Combined Brick/ Castable	4-Layer Insulation (Ref. 4)
Heater Vessels (Including Matrix)	.44	.35	.31	.39	.42
Manifolds	.31	.14	.09	.16	.25
Support Structure	.08	.05	.05	.07	.06
Other	.17	.16	.16	.17	.17
Total Relative Cst.	1.00	.70	.61	.79	.90

Does not include collector manifold(s) from radiant boiler

TABLE 5

HTAH Cost Comparison for Large and Small Manifold Design, Lowest Risk Brick Insulation

HTAH Component	Large Manifold System	Small Manifold System
Heater Vessels (Including Matrix)	0.44	0.44
Manifolds	0.31	0.23
Support Structure	0.08	0.07
Other	0.17	0.17
Total	1.00	0.91

Does not include collector manifolds(s) from radiant boiler

TABLE 6

Outlet Fluid Temperature Variation and Maximum Bottom of Matrix Solid Temperatures from SCAMP Computer Code Runs

	Total Variation in Outlet Air Temperature K (F)	Total Variation in Outlet Gas Temperature K (F)	Range of Individual Heater Maximum Bottom of Matrix Solid Temperature * K (F)
Large Manifolds	24 (44)	16 (29)	1336-1393 (1944-2047)
Small Manifolds	50 (90)	31 (56)	1279-1446 (1843-2143)
Small Manifolds with control by Air/Gas Phase Duration	51 (92)	21 (38)	1379-1451 (2023-2152)

*Maximum Bottom of Matrix Temperature of at least 1400 K (2060 F) is desired for each individual heater to promote effective seed/slag drainage

TABLE 7

Electrical Conductivity of Air Stream with Various Levels of Potassium Contamination

Air Stream Temperature	wt % K			
	0.001%	0.01%	0.1%	1.0%
1550 K	$\mu_e = .146$ $n_e = 7.88 \times 10^{14}$ $\sigma = 1.84 \times 10^{-5}$	$\mu_e = .146$ $n_e = 2.43 \times 10^{15}$ $\sigma = 5.68 \times 10^{-5}$	$\mu_e = .138$ $n_e = 7.78 \times 10^{15}$ $\sigma = 1.72 \times 10^{-4}$	$\mu_e = .104$ $n_e = 2.91 \times 10^{16}$ $\sigma = 4.85 \times 10^{-4}$
1700 K	$\mu_e = .151$ $n_e = 5.62 \times 10^{15}$ $\sigma = 1.36 \times 10^{-4}$	$\mu_e = .150$ $n_e = 1.76 \times 10^{16}$ $\sigma = 4.24 \times 10^{-4}$	$\mu_e = .145$ $n_e = 5.65 \times 10^{16}$ $\sigma = 1.31 \times 10^{-3}$	$\mu_e = .111$ $n_e = 2.13 \times 10^{17}$ $\sigma = 3.79 \times 10^{-3}$
1850 K	$\mu_e = .156$ $n_e = 3.14 \times 10^{16}$ $\sigma = 7.84 \times 10^{-4}$	$\mu_e = .155$ $n_e = 9.90 \times 10^{16}$ $\sigma = 2.46 \times 10^{-3}$	$\mu_e = .152$ $n_e = 3.17 \times 10^{17}$ $\sigma = 7.72 \times 10^{-3}$	$\mu_e = .117$ $n_e = 1.19 \times 10^{18}$ $\sigma = 2.22 \times 10^{-2}$
2000 K	$\mu_e = .162$ $n_e = 1.40 \times 10^{17}$ $\sigma = 3.64 \times 10^{-3}$	$\mu_e = .161$ $n_e = 4.43 \times 10^{17}$ $\sigma = 1.14 \times 10^{-2}$	$\mu_e = .156$ $n_e = 1.42 \times 10^{18}$ $\sigma = 3.54 \times 10^{-2}$	$\mu_e = .123$ $n_e = 5.22 \times 10^{18}$ $\sigma = 1.03 \times 10^{-1}$

Stream Saturated with K_2SO_4

Pressure = 10 atm

	1550 K	1700 K	1850 K	2000 K
Max. wt % K in gas:	0.0078%	0.050%	0.23%	0.77%

Interpolated values for maximum σ at each temperature:

	1550 K	1700 K	1850 K	2000 K
Max. σ =	5.03×10^{-5}	9.33×10^{-4}	1.13×10^{-2}	9.12×10^{-2}

FIGURES

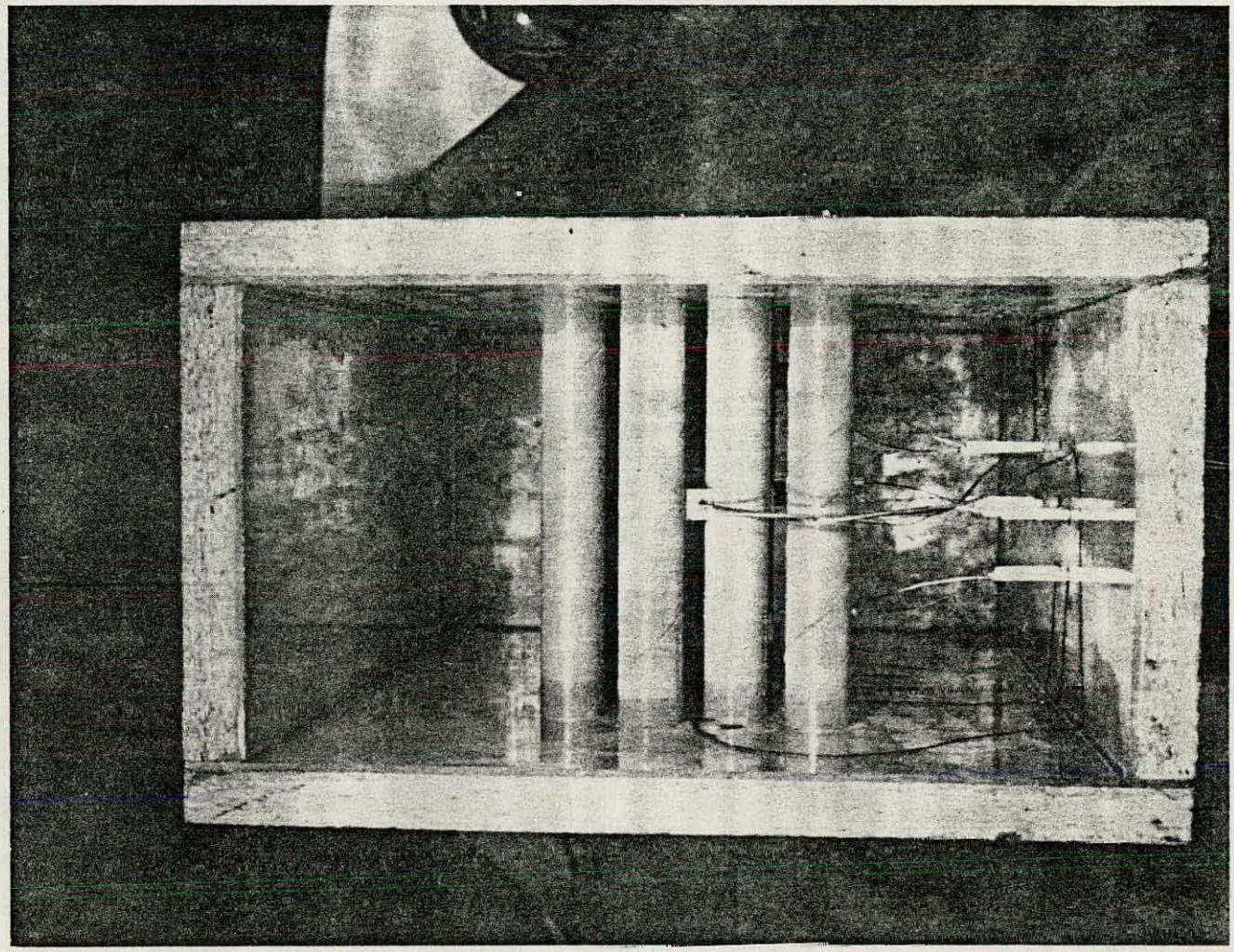

FIGURE 1 MOLD FOR CASTING MATRIX SUPPORT FOR MTF

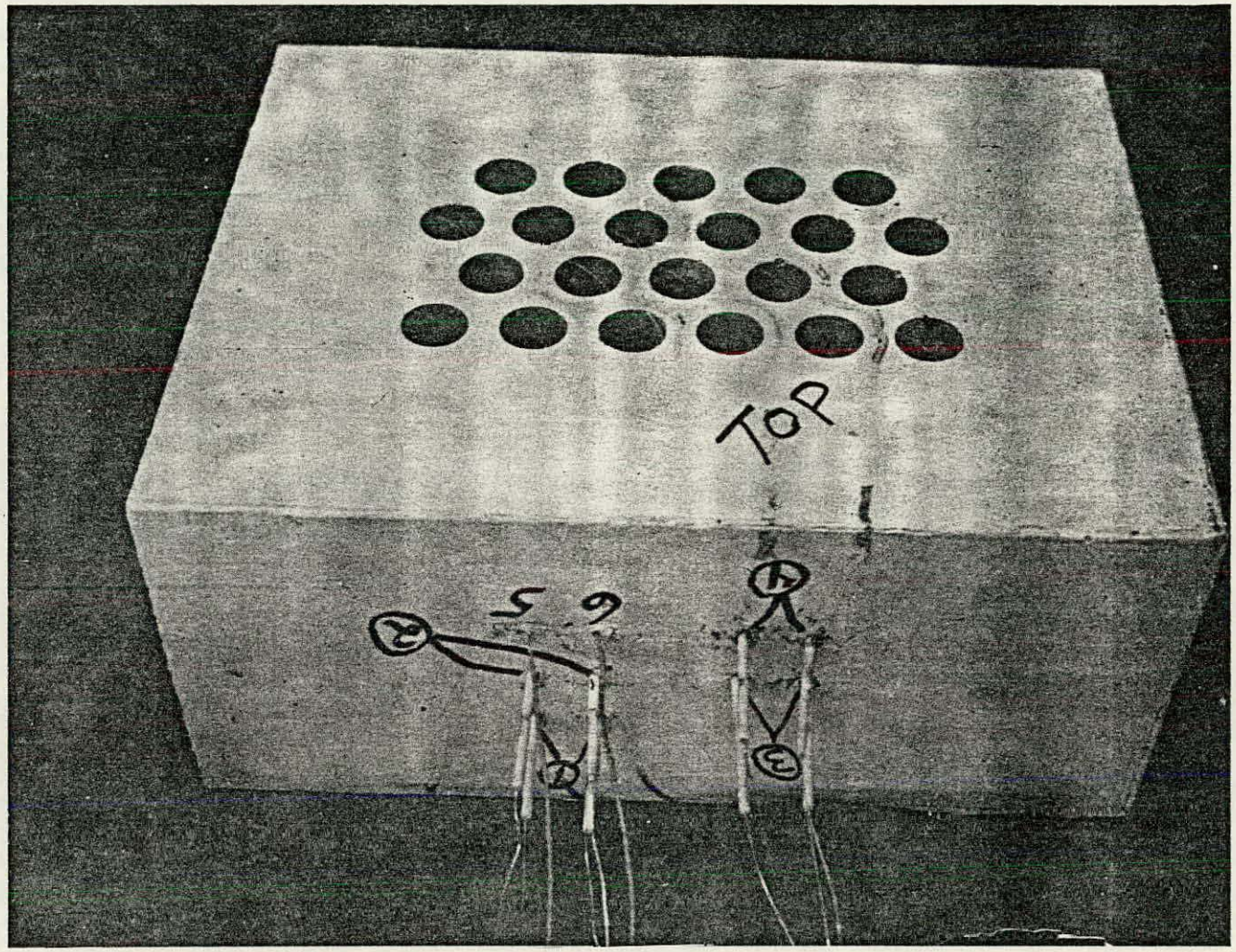

FIGURE 2 CASTABLE SPINEL MATRIX SUPPORT BRICK FOR MTF

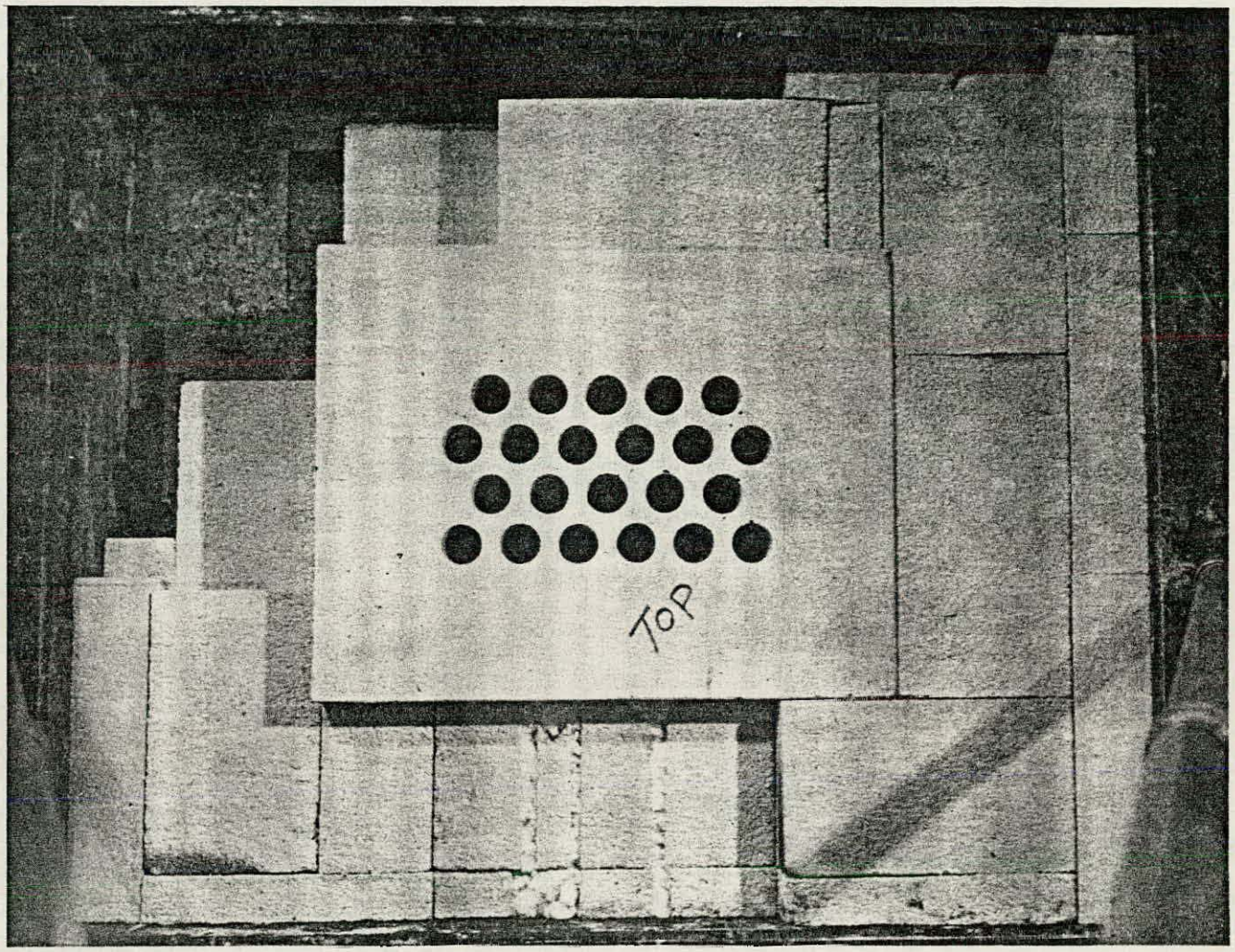

FIGURE 3 MATRIX SUPPORT BRICK BEING INSTALLED IN MTF

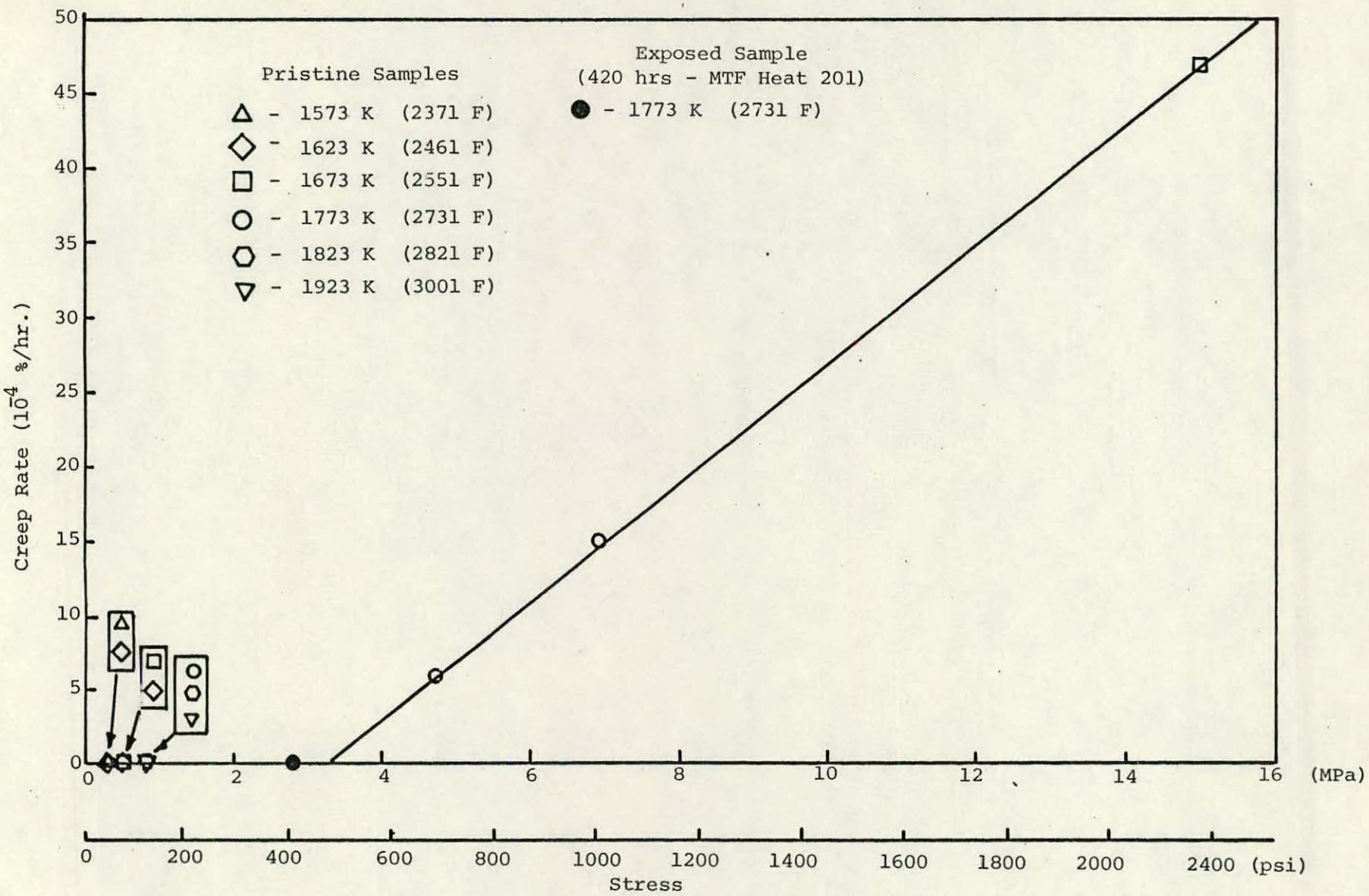

FIGURE 4. STEADY STATE CREEP RATE OF CORHART X-317
(DATA FROM MONTANA TECH MEASUREMENTS)

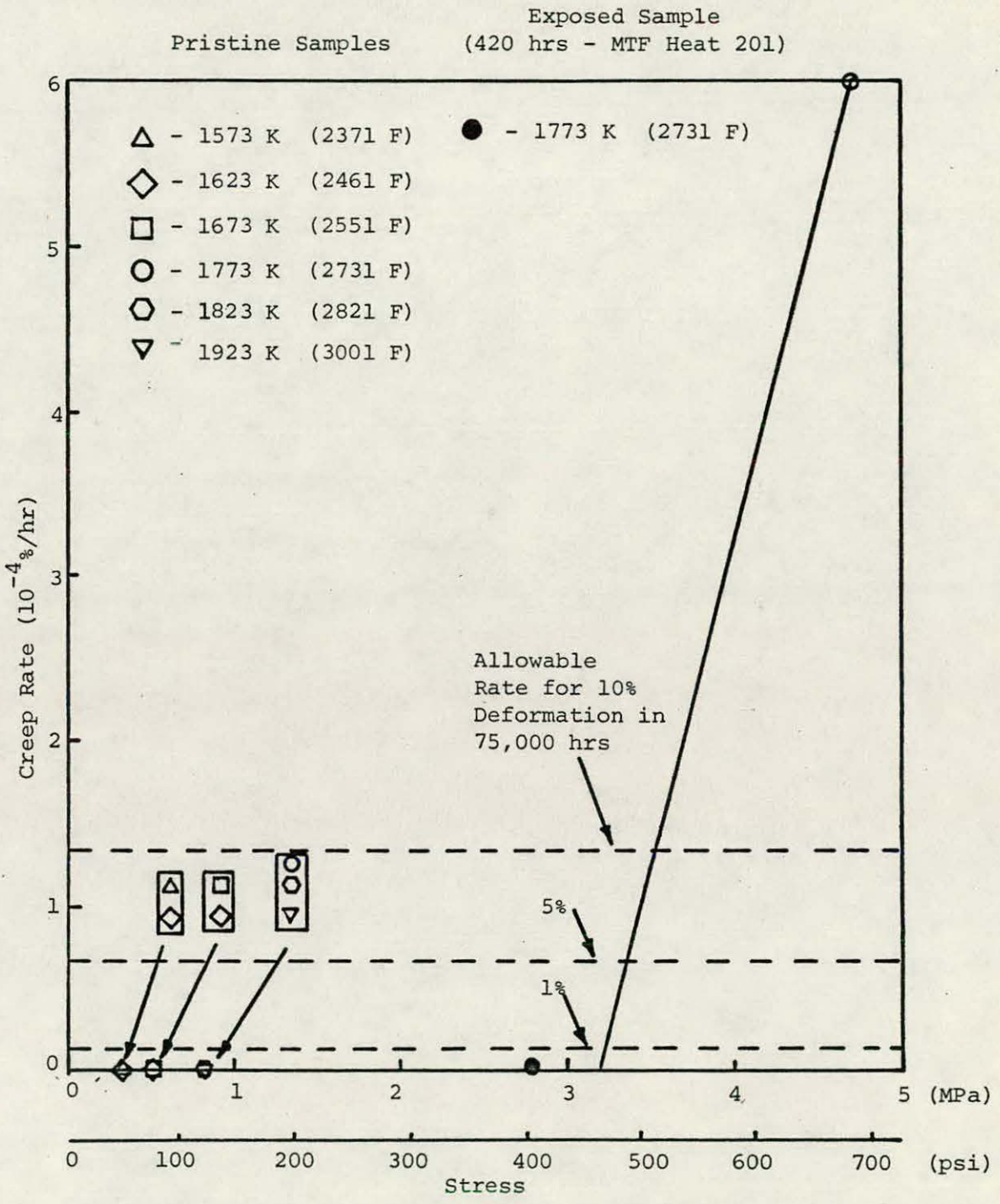

FIGURE 5. STEADY STATE CREEP RATE OF CORHART X-317 COMPARED WITH ALLOWABLE CREEP RATES OVER LIFE OF HTAH MATERIALS (DATA FROM MONTANA TECH MEASUREMENTS)

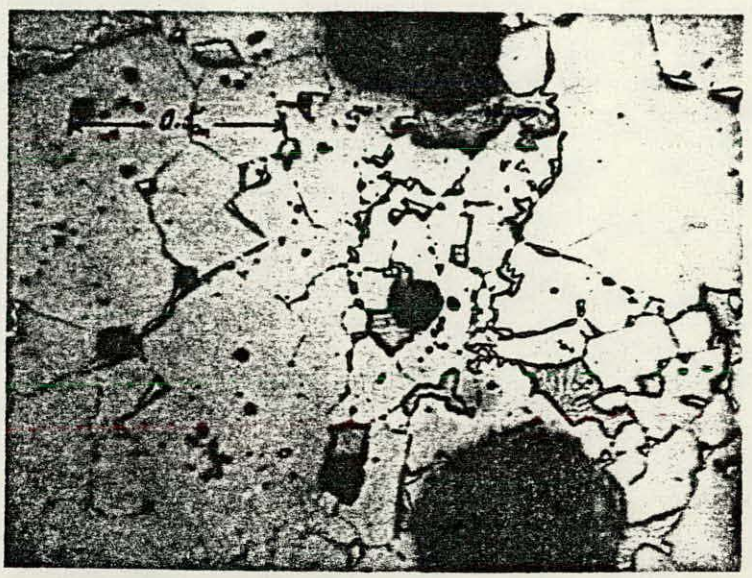

Figure 6
Unreacted interior of LS812 - 72X

Figure 7

Hot face of LS812 from Valve Test 3

Figure 8

Hot face of LS812 from Valve Test 3
Showing Penetration Solution or Refractory

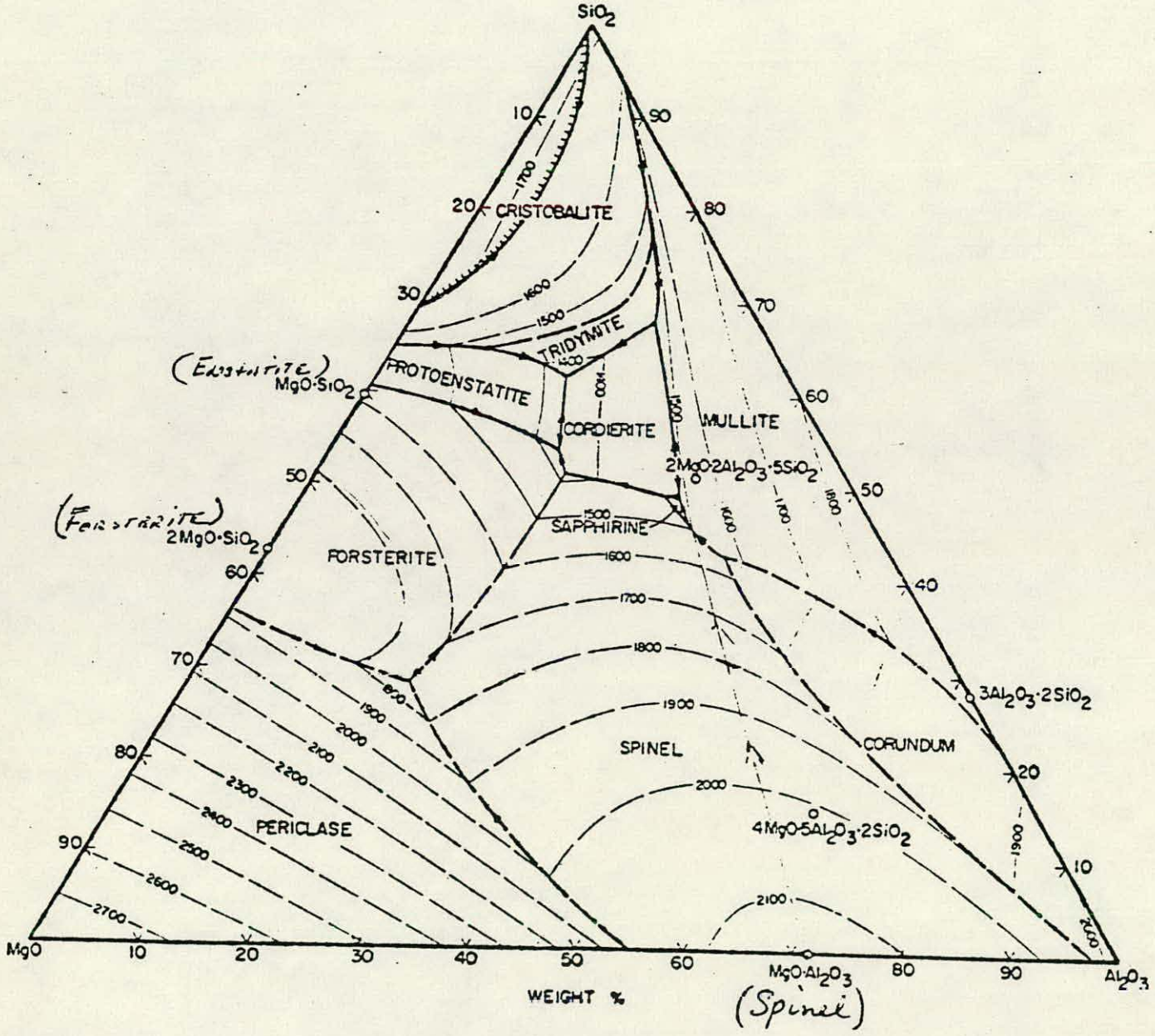

Figure 9. Phase Diagram for the System MgO-Al2O3-SiO2

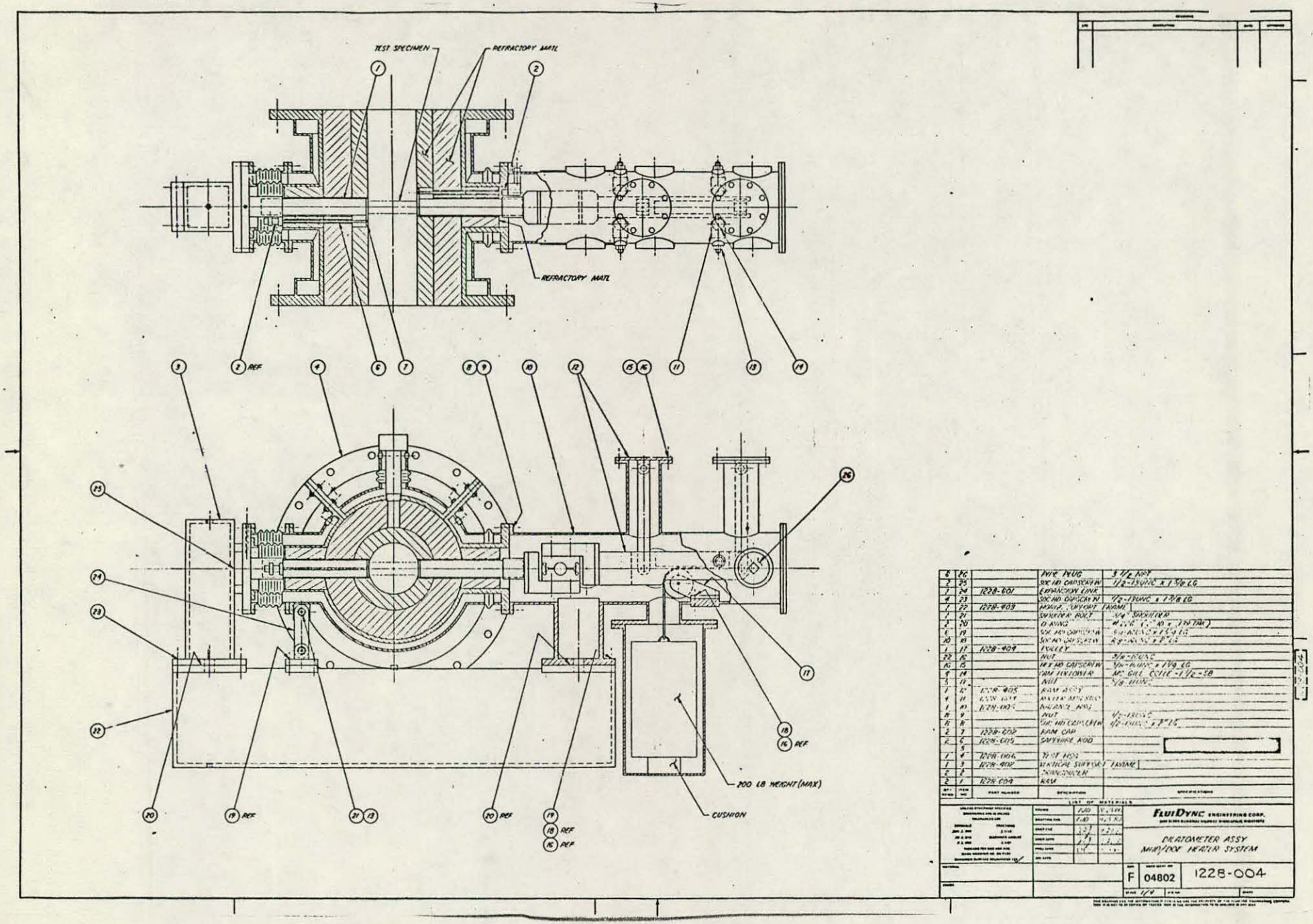

FIGURE 10. DILATOMETER ASSEMBLY DRAWING

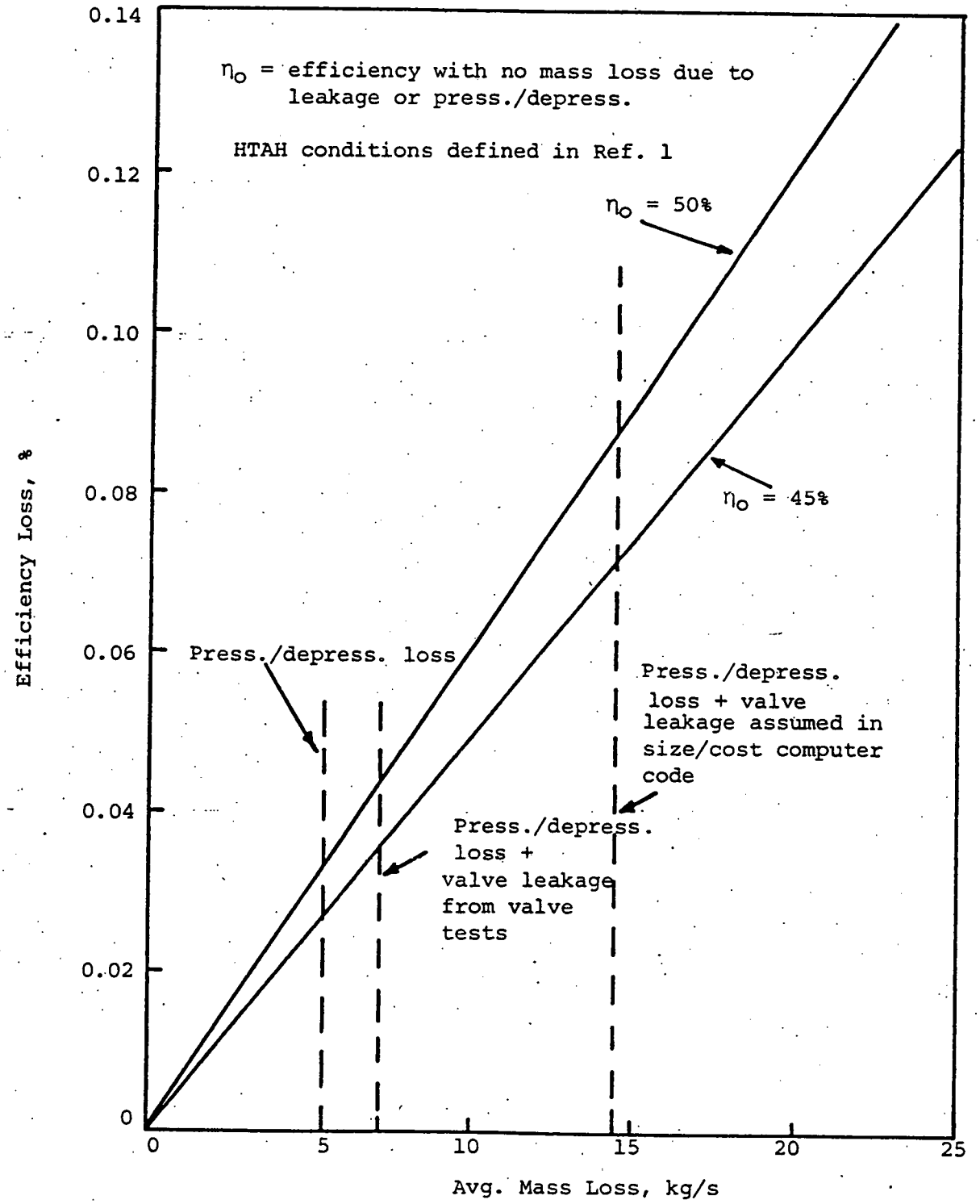

FIGURE 11. LOSS IN OVERALL PLANT EFFICIENCY DUE TO HTAH VALVE LEAKAGE AND PRESSURIZATION/DEPRESSURIZATION MASS LOSS FOR 1000 MW_e PLANT

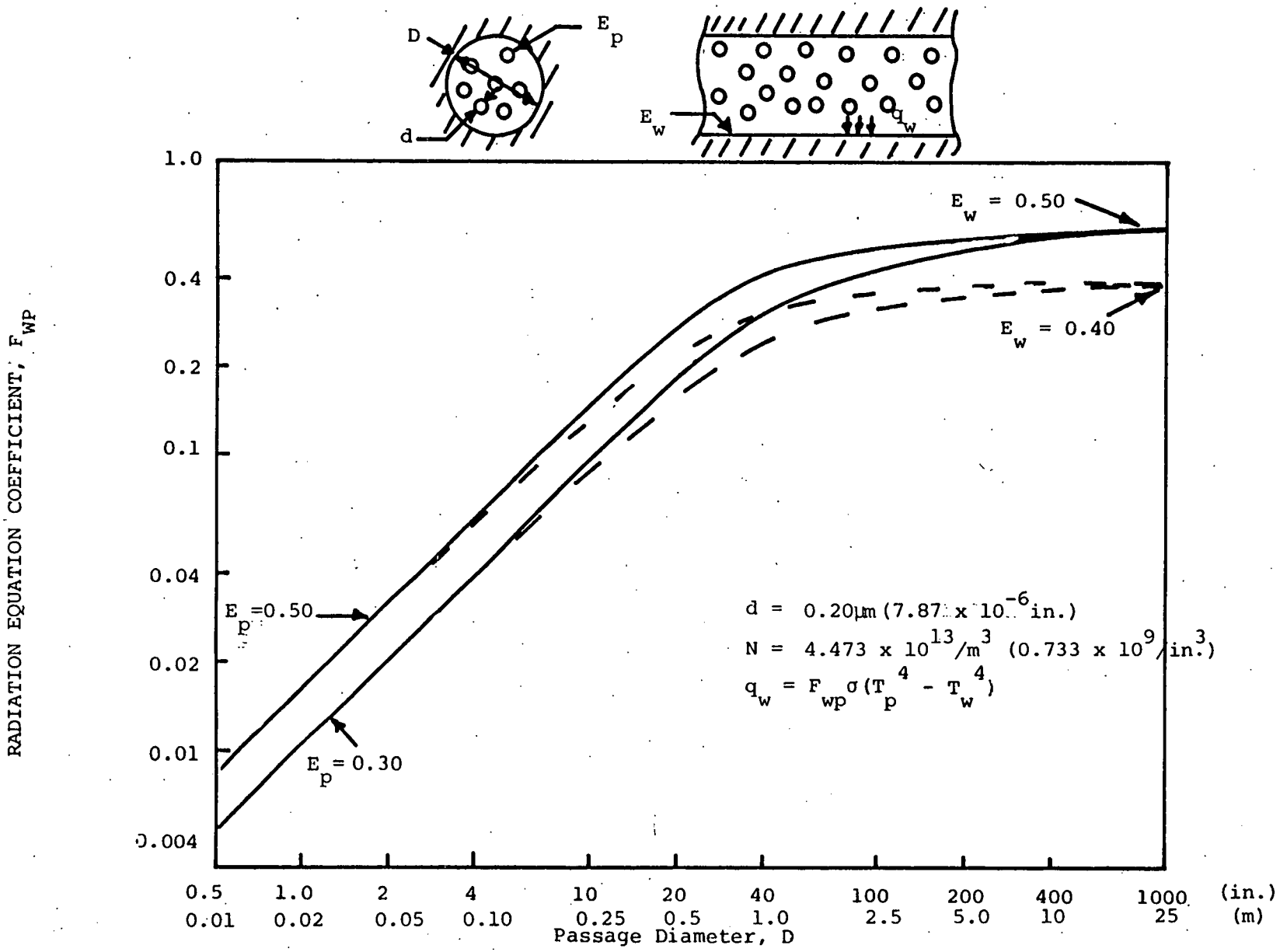

FIGURE 12 INTERCHANGE FACTOR OF CYLINDRICAL WALL WITH RESPECT TO PARTICLES FOR MHD CHANNEL EXHAUST GAS

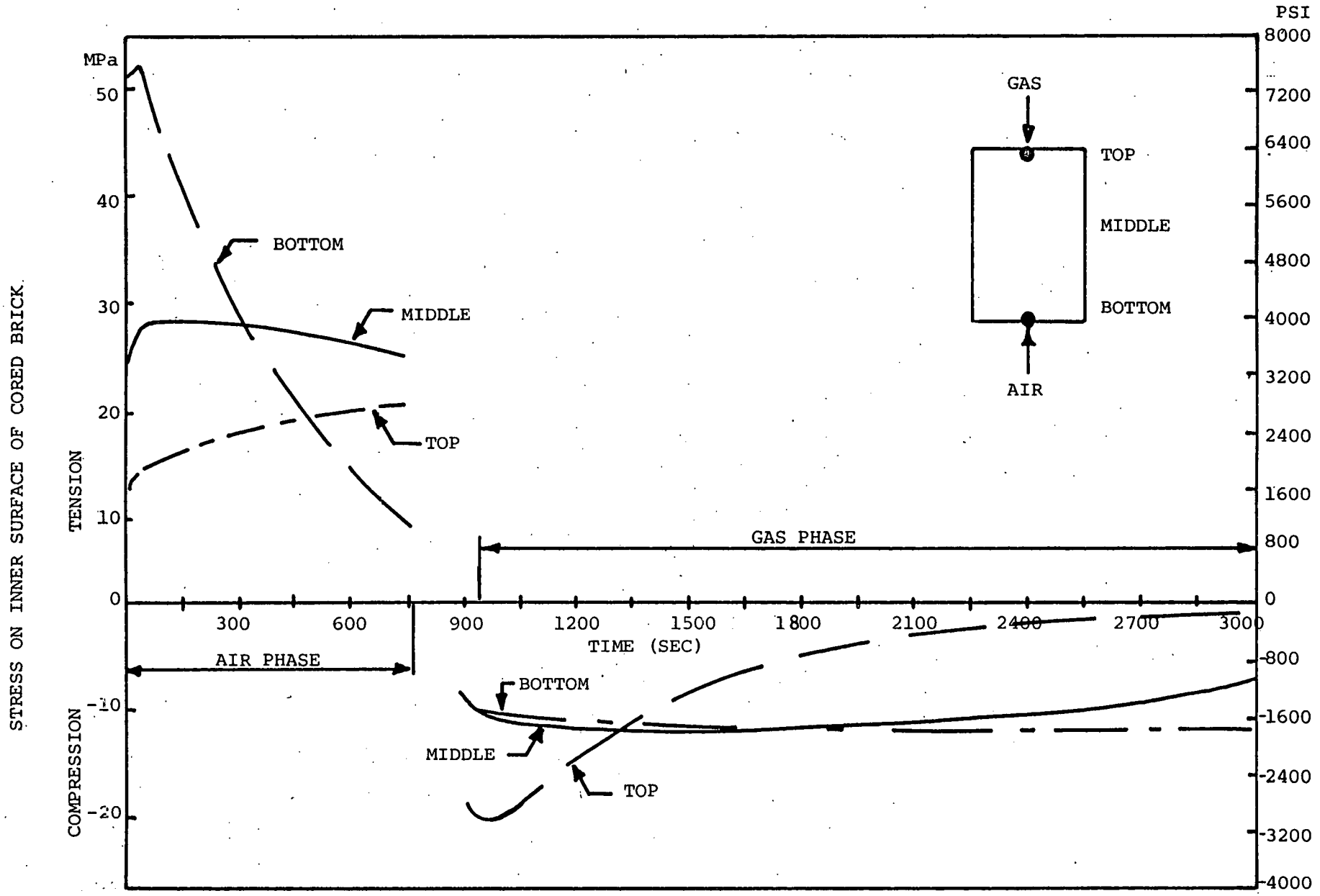

FIGURE 13. THERMAL STRESS AT VARIOUS AXIAL POSITIONS IN MATRIX

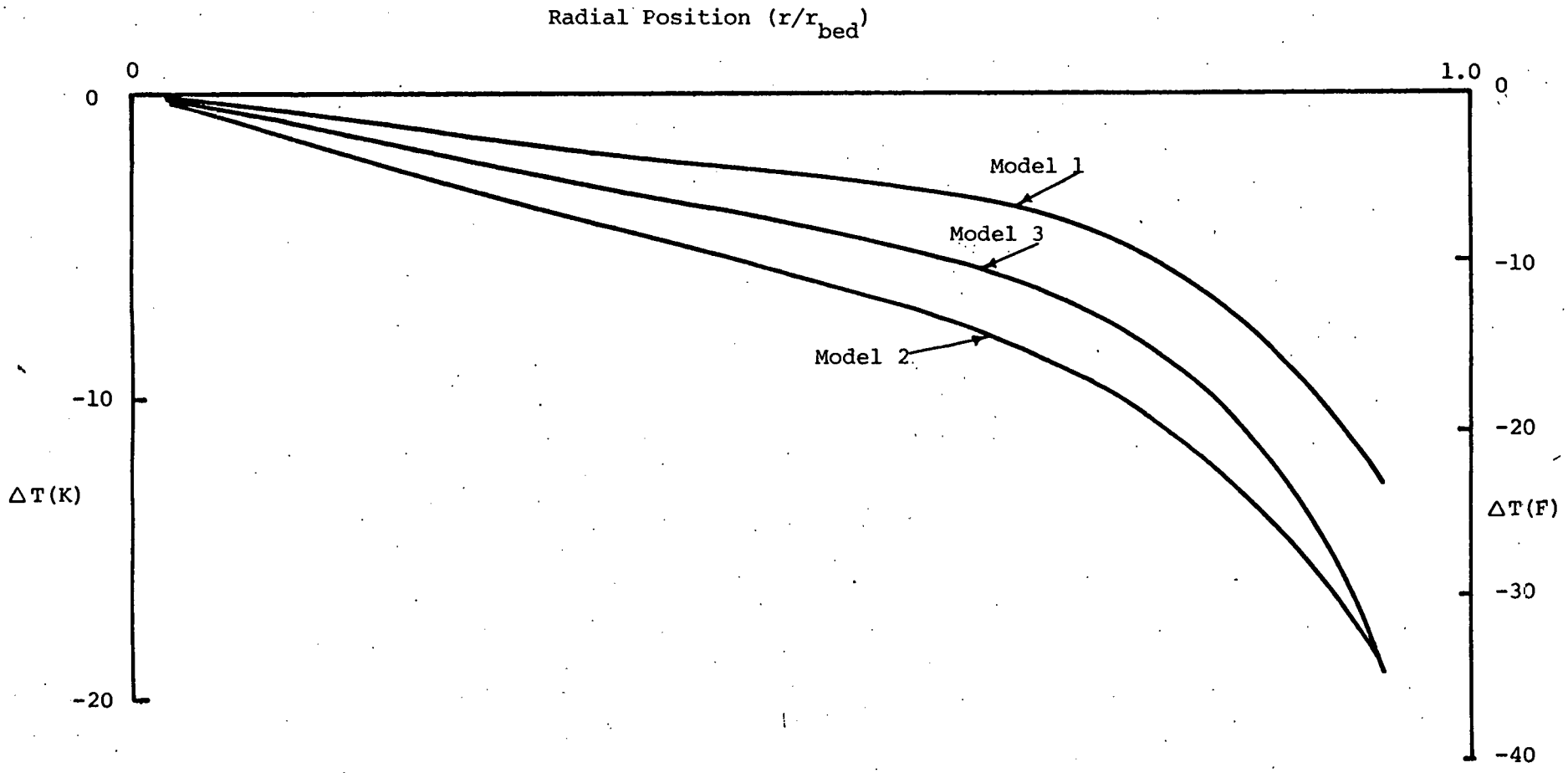

FIGURE 14. END OF GAS PHASE TEMPERATURE DIFFERENCE FOR RADIAL ELEMENTS, STRHEX

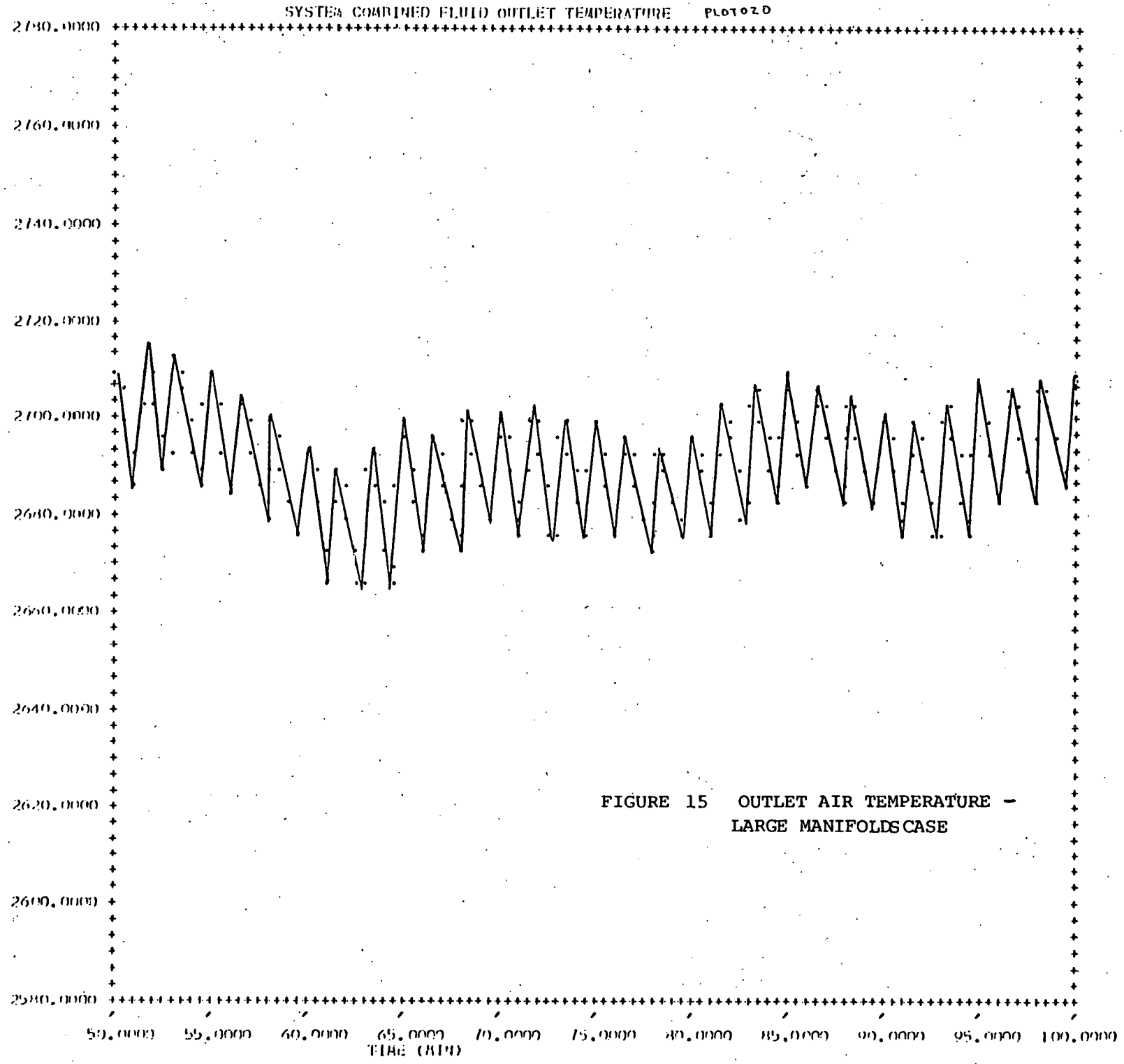

FIGURE 15 OUTLET AIR TEMPERATURE – LARGE MANIFOLDS CASE

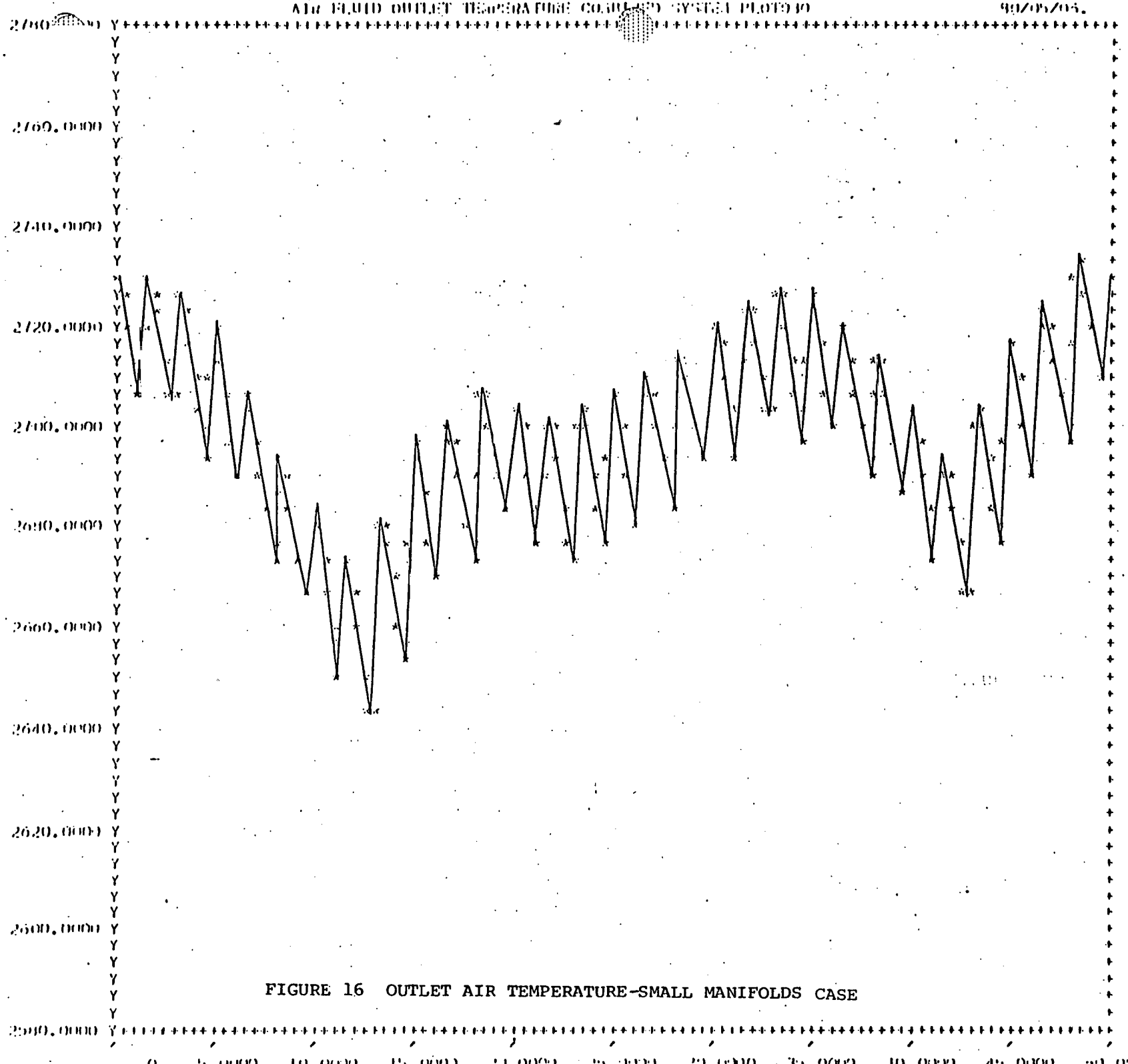

FIGURE 16 OUTLET AIR TEMPERATURE-SMALL MANIFOLDS CASE

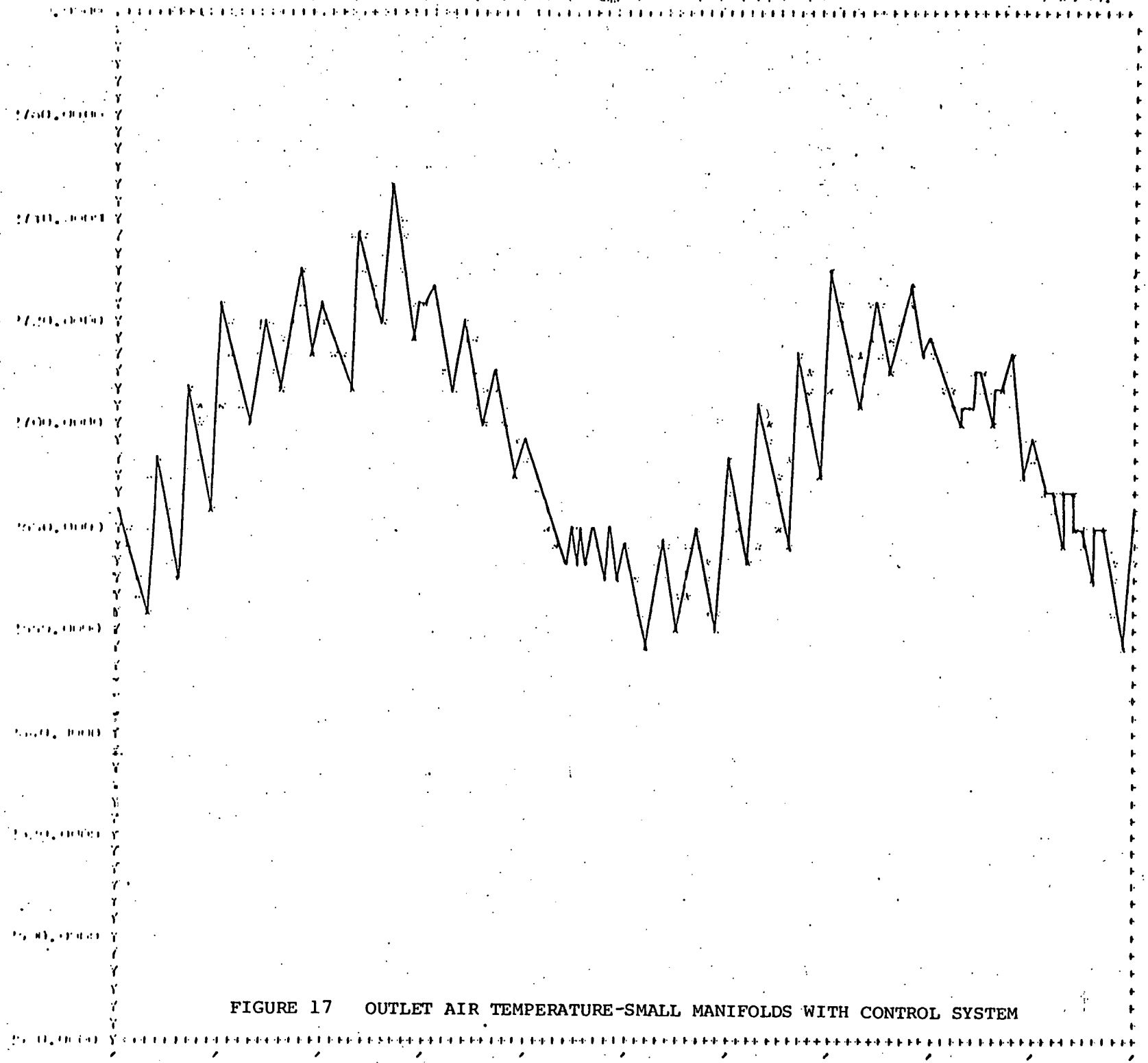

FIGURE 17 OUTLET AIR TEMPERATURE-SMALL MANIFOLDS WITH CONTROL SYSTEM

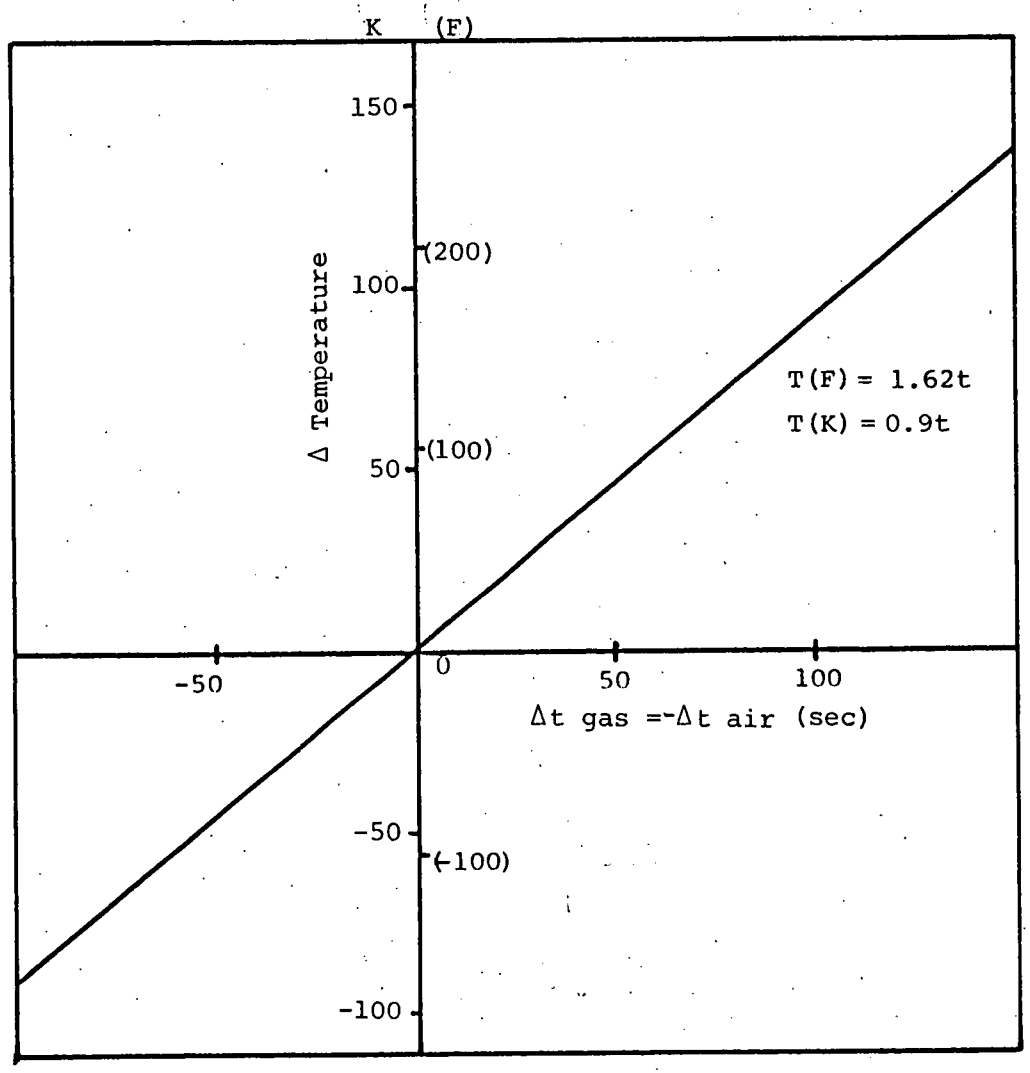

FIGURE 18. CHANGE IN MAXIMUM BOTTOM OF BED SOLID TEMPERATURE WITH CHANGE IN GAS-AIR CYCLE TIME FROM STRHEX

APPENDIX

Outline Specification

Fused grain high density spinel brick special shapes

1.0 Inspection Lots

2.0 Dimensions and Tolerances

2.1 All dimensions shall be within the tolerances specified by the drawings.

2.2 Pilot order: Each brick shall be inspected. Production order: Inspect by 2.5 AQL II single-normal per MIL-STD-105D. Thus 80 bricks will be inspected in each lot of 1000 bricks. Lot will be accepted if 5 or fewer bricks are rejected. Lot will be rejected if 6 or more bricks are rejected.

3.0 Surface Characteristics

3.1 All die flash and feather edges must be removed.

3.2 All surfaces must be smooth and free of loose grains.

3.3 Honeycomb surface area must not exceed 1 sq. in. cumulative per brick.

3.4 Bricks with visible open cracks (width 0.002 inch or greater) not acceptable.

3.5 Hairline cracks (width less than 0.002 inch) of cumulative length 1 inch per brick will be acceptable. Isolated cracks less than 1/8 inch long will not be included in the cumulative length.

3.6 Bricks with a network of surface cracks or surface checking not acceptable.

3.7 Bricks having surface stains with indented or glassy areas not acceptable.

3.8 Visual standards will be provided for honeycomb surfaces.

3.9 Pilot order: Each brick shall be inspected.
Production order: Each brick shall be inspected.

4.0 Density and Internal Structure

4.1 Density shall be in range 73.0 to 79.0 percent of theoretical (4.00 gm/cc). (2.92 - 3.16 gm/cc or 182 - 197 pcf).

4.2 Density variation within any brick shall not exceed $\pm$0.10 gm/cc when measured with a sample containing no more than 10% of the brick volume.

4.3 Density may be measured by ASTM C20-46(1967) or equivalent methods. The C20-46(1967) test will be modified to include a 10 second exposure to 30 psi compressed air from a 1/32" orifice at a distance of 6" to blow water droplets from inside surface of holes.

4.4 Bricks with pores having any dimension greater than 1/8 inch not acceptable.

4.5 Internal structure must have uniform texture.

4.6 Bricks with lamination cracks longer than 1/2 inch not acceptable.

4.7 Bricks with visible black coring or internal discoloration not acceptable.

4.8 Pilot order: Inspect minimum of 4 bricks per lot.
Production order: Inspect minimum of 2 bricks from each lot selected for inspection.

5.0 Chemical Composition

5.1	Al_2O_3	-	70.0% minimum
	MgO	-	28.00
	Al_2O_3 + MgO	-	99% minimum
	Na_2O	-	0.60% maximum
	SiO_2	-	0.10% maximum
	Fe_2O_3	-	0.10% maximum
	TiO_2	-	0.05% maximum
	C	-	0.05% maximum
	S	-	0.05% maximum
	LO I	-	0.20% maximum

5.2 Test method: ASTM C573-65 or equal.

5.3 Pilot order: Inspect minimum of 1 brick per lot.
Production order: Inspect minimum of 1 brick from each lot selected for inspection.

6.0 Reheat Shrinkage and Weight Loss

6.1 Reheat shrinkage shall not exceed 0.5%.

6.2 Reheat weight loss shall not exceed 0.1%.

6.3 Test method: ASTM C113-61 modified as follows:

6.3.1 Test specimens shall be special shapes

6.3.2 Weight of each specimen shall be measured before and after test to within $\pm$0.05 gm. Weights and percent weight changes shall be reported.

6.3.3 Furnace shall be gas fired with oxidizing atmosphere maintained at all times.

6.3.4 Heating Schedule C shall be followed except that the maximum temperature shall be 3040°F and attained after 6 hours. The maximum temperature shall be held for 10 hours.

6.3.5 Optical pyrometer readings made by sighting directly on the specimen may be used instead of thermocouple readings.

6.4 Pilot order: Inspect minimum of 1 brick per lot. Production order: Inspect minimum of 1 brick from each lot selected for inspection.

7.0 High Temperature Deformation

7.1 Linear deformation shall not exceed 2.5% in 400 hours at 3000°F.

7.2 Test method: ASTM C16-67 modified as follows:

7.2.1 Specimen shall consist of a vertical column of cored bricks. Height of column (parallel to holes) shall be approximately 9 in.

7.2.2 Load shall be 15 psi of solid material surface.

7.2.3 Furnace shall be gas fired with oxidizing atmosphere maintained at all times.

7.2.4 Heat Schedule No. 7 shall be followed except that the maximum temperature (3000°F) shall be held for 400 hours.

7.2.5 The length of the test specimen shall be continuously monitored, or the test shall be interrupted at intervals no longer than 100 hours and the length of the specimen measured.

7.3 Pilot order: Inspect minimum of 3 bricks per lot. Production order: No inspection planned.

8.0 Cold Crushing Strength

8.1 Cold crushing strength shall be measured by ASTM C133-55 (1961) modified as follows:

8.1.1 The test specimens shall be cut from special shapes to produce flat parallel faces.

8.1.2 The failure stress shall be calculated on the basis of the solid material area.

8.1.3 Five specimens selected at random shall be tested.

8.1.4 The stress at failure for each specimen and the average value shall be reported.

8.2 Individual values of cold crushing strength shall not be less than 3000 psi.

8.3 The average value of cold crushing strength shall not be less than 6000 psi.

8.4 Pilot order: Inspect minimum of 5 pieces per lot. Production order: Inspect minimum of 5 pieces from each lot selected for inspection.

9.0 Thermal Shock Resistance

9.1 Reduction in modulus of rupture as a result of thermal shock damage shall not exceed 25% after 20 thermal cycles.

9.2 Samples shall be bars cut from two pieces. Bars shall be cut from side surfaces of the piece with length equal to the length of the brick. A total of 12 test bars will be prepared. The cross section width and thickness of the test bars shall be approximately 1 inch by 0.55 inch, each selected to include two holes symmetrically placed along the one inch width for cored bricks.

9.3 Three samples from each of the two bricks shall be heated to 1500°F, then cooled to 500°F or less at a rate of at least 200°F/minute for 20 complete cycles. Furnace shall be gas fired with oxidizing atmosphere maintained at all times.

9.4 Modulus of rupture at room temperature shall be measured by ASTM C133-55 (1961) modified as follows:

9.4.1 The 12 bars of Para. 9.2 shall be tested. Six of these bars will have been temperature cycled according to Para. 3.3.

9.4.2 The loading and support apparatus shall be adjusted to the specimen size, nominally 1/2 inch thick x 1 inch wide x 3 inches long.

9.4.3 The tension surface shall be the uncut surface of the brick (outer hexagonal face).

9.4.4 Individual values of modulus of rupture shall be reported.

9.4.5 Average values of modulus before and after temperature cycling shall be calculated by omitting the lowest individual values for each set of six specimens, and averaging the remaining five values.

9.5 The average value of modulus of rupture before temperature cycling shall not be less than 1600 psi.

9.6 The average value of modulus of rupture after temperature cycling shall not be less than 1200 psi.

9.7 Pilot order: Inspect minimum of 2 bricks per lot. Production order: Inspect minimum of 2 bricks from each lot selected for inspection.